When do leading and rear edges of the range shift slower or faster than climate? Insights from a mathematical model

Matthieu Alfaro[1], Gaël Raoul[2], and Ophélie Ronce[3@]

[1]Université de Rouen Normandie, CNRS, Laboratoire de Mathématiques Raphaël Salem, Saint-Etienne-du-Rouvray, France.

[2]CMAP, CNRS, Ecole polytechnique, I.P. Paris, 91128 Palaiseau, France.

[3]ISEM, Univ Montpellier, CNRS, IRD, Montpellier, France.

[@]Corresponding author: ophelie.ronce@umontpellier.fr

Short running title: Predicting niche and range shifts under climate change

Keywords: niche evolution, spread, expansion, contraction, asexual species, dispersal, mutation, extinction, climatic debt, local adaptation

Abstract word count: 291

Impact statement word count: 288

Main text word count: 6367

Abstract

Climatic spatial gradients often result in the evolution of locally adapted phenotypic clines. Such gradients should shift through time under climate warming. Species can then persist (i) by tracking through space the range of climatic conditions to which they are already adapted to, (ii) by staying put and evolving new trait values allowing adaptation to new conditions, or (iii) by any combination of migration and evolution, with varying consequences for the position of the rear and leading edge of their range in a changing climate. We here use previously developed mathematical results to predict the speed at which such rear and leading edge move in an asexual species adapting to an environmental gradient that shifts in space and time. We jointly model changes in the distribution of the species abundance through space and changes in the distribution of phenotypic values defining its climatic niche. As in previous studies, we find that there is a critical climate change velocity beyond which the species cannot persist. We can however define several other types of critical climate change velocities, which allow predicting when the leading edge shifts faster or slower than climate change, and when the species persists at its rear edge. We derive predictions along a one-dimensional spatial gradient and in two dimensions. In the latter case, we predict that the direction of faster spatial spread at the edge of the range is not always the direction of faster climate change. We also predict when a local disturbance in the latitudinal climatic gradient, e.g. generated by a mountain, can stop the spread of the population despite climate warming. Conversely, local improvement of population growth, as may occur in protected areas, can allow persistence at the rear edge under faster rates of climate changes.

Impact statement: The geographical distribution of many species is already altered by contemporary climate change. Observed spread towards cooler climates and extinction at the warm margin of the range are consistent with the expectation that species track the climatic conditions to which they are already adapted. Yet, despite this global signal of climate change impact on biodiversity, our understanding of what drives the large diversity in observed range shifts remains limited. Some species indeed spread faster or slower than expected based on the idea of climate tracking and range shifts patterns frequently differ between the warm and cold margins of the species range. We here use a mathematical model to predict how evolutionary adaptation to new climates along with climate tracking may modify our expectations regarding range shifts under climate warming. Our model suggests that shifts in the position of the cold margin of the range will be typically faster than shifts at the warm margin, consistently with many observations. We also predict that different species can survive climate warming through a diversity of patterns combining range shifts and niche evolution: some spread faster and others slower than climate change at their cold margin, some persist and others die out at their warm margin, depending on their dispersal capacity, evolutionary potential and speed of climate warming. Our simple mathematical model thus shows that rapid evolution of species climatic niches can already generate a large diversity of types of range shift in a warming climate and that the expectation of a simple climate tracking may be too simplistic, underestimating the resilience capacity at the warm margins and either overestimating or underestimating the capacity for spread at the cold margin, with important consequences for management of biodiversity in a changing climate.

1 Introduction

Changes in spatial distribution consistent with impacts of contemporary climate change, such as poleward and upslope range shifts, have now been documented for a large number of species in many ecosystems (see Chen et al., 2011; Lenoir and Svenning, 2015; Lenoir et al., 2020). Direction, speed and drivers of these shifts are however highly idiosyncratic: they vary among species, but also, for the same species, between different range margins, and depending on whether changes in abundances within the range or changes in the position of range limits are considered. Fossil records similarly show large variation in patterns and speeds of species range shifts following periods of past climate change (Willis and MacDonald, 2011; Ordonez, 2013). In both contemporary and past warming periods, velocities at the trailing edge are often much lower than at the leading edge (Willis and MacDonald, 2011; Ordonez, 2013; Lenoir and Svenning, 2015). The speed of changes at both margins is also frequently lower than expected based on climate change (Lenoir and Svenning, 2015), but changes can also be faster than (Ordonez, 2013), or in the opposite direction to (Lenoir et al., 2010), shifts in temperature isotherms. This large variation remains largely unexplained. Attempts to predict patterns and speed of range shifts from species traits in meta-analyses of empirical data (Angert et al., 2011; MacLean and Beissinger, 2017; Platts et al., 2019; Lenoir et al., 2020; Beissinger and Riddell, 2021) have been met with moderate success. Many species in particular seem to persist in localities where the climate has become unfavourable, a pattern described as a climatic debt (Bertrand et al., 2016; Gaüzère et al., 2017). While this persistence may only be transient, hiding future local extinction, paleorecords of plant species distributions offer a more optimistic view, suggesting an important role for microrefugia and evolutionary adaptation in helping species holding on at their rear edge through warming periods (Willis and MacDonald, 2011). Our aim here is to develop new mathematical models to better understand and predict patterns of species range shifts in the context of climate change, when species can both track favourable climate through space and evolve new thermal niche limits. Our hypothesis is that a better understanding of evolutionary responses to climate change and their interaction with spatial spread should help better predicting the observed diversity of range shifts in the context of contemporary and past climate changes.

The rich theory about mathematical models of spatial spread has been used to generate predictions about spatial shifts in distributions in the context of climate change. Simple models of diffusion in homogeneous space (Fisher, 1937; Kolmogorov et al., 1937) predict that life history traits affecting the dispersal distance and the population growth rate at low density should determine the velocity of expanding margins, a prediction having received weak empirical support in the context of contemporary climate change (Angert et al., 2011). Spatial spread in the context of climate change differs from the spread of an invasive species in an homogeneous environment in that the climate varies through space

and the species can survive only within its climatic niche. Models of "moving habitat" (Potapov and Lewis, 2004; Berestycki et al., 2009; Cobbold and Stana, 2020) describe such a niche with fixed limits and predict that the rate of both spread of the leading edge and contraction of the trailing edge are set by the climate change velocity. Above a critical climate velocity, the species fails to track in space its preferred climate and goes extinct globally. Consistently with these predictions, climate velocity is tightly linked to the velocity of movement in some species, but this relationship is much more loose for others (Chen et al., 2011; Lenoir et al., 2020).

Several important biological factors are left out by the previous mathematical models and may explain why they fail at predicting the observed diversity of range movements in response to climate change. These models ignore the existence of genetic variability in the adaptation to local climate within the species range (see Peterson et al., 2019) and the ability of species to evolve new niche limits. There is increasing recognition that spatial spread can be slowed down or accelerated by fast evolution accompanying expansion in the context of climate change (Diamond, 2018; Nadeau and Urban, 2019; Wellenreuther et al., 2022), as exemplified by the evolution of higher dispersal capacity or higher mutation load at the expanding edge (Peischl and Gilbert, 2020). Joint evolution of local adaptation and spatial spread has also to be considered when expanding species adapt to environments that are variable in space, such as climatic gradients across elevation or latitude (Davis et al., 2005). Local adaptation describes the evolution of local values of phenotypic traits that confer high fitness in a specific locality within the range, but not in other parts of the range, and is a pervasive feature of natural populations (Peterson et al., 2019). Evolution of locally-adapted flowering phenology seems in particular to have facilitated the spread of several plant species colonizing climatic gradients in the current context of climate warming (Colautti and Barrett, 2013; Lustenhouwer et al., 2018). A number of simulation models have described the joint evolution and spread of one or several species along climatic gradients shifting in space and time due to climate change (e.g. Kubisch et al., 2013; Hargreaves et al., 2015; Thompson and Fronhofer, 2019; Weiss-Lehman and Shaw, 2020; Moran, 2020), reaching quite different conclusions. As these simulation models differ in many specific assumptions (see discussion in Moran, 2020), it is difficult to lay out the general principles and expectations about the effect of evolution of local adaptation on patterns of range changes in the context of climate change.

Mathematical models have also been developed to describe a species spreading in geographical space and evolving in phenotypic space along some environmental gradient, with different phenotypic values maximizing population growth rates at different points along this gradient, and a shifting gradient mimicking climate change (Pease et al., 1989; Polechová et al., 2009; Duputié et al., 2012; Aguilée et al., 2016). These models are related to a larger body of evolutionary biology theory (Kirkpatrick and Barton, 1997; Case and Taper, 2000; Polechová and Barton, 2015; Polechová, 2018), connecting key questions

about the evolution of species ranges and of niches. These models assume sexual reproduction and predict three possible ultimate outcomes when a species adapt to such a shifting spatial gradient: (i) the species may go extinct everywhere, (ii) it may evolve a finite range, which shifts with climate change, with the same speed at the leading and trailing edge, (iii) the species may ultimately spread and adapt to the entire gradient. Although these models allow change in niche limits, some predict that climate change will not cause niche evolution, but rather the spatial tracking of the favourable climate through range shifts as fast as climate change (Pease et al., 1989; Duputié et al., 2012). Yet, this prediction does not appear to be particularly robust, as, for instance, relaxed competition at the front may result in leading edge shifting faster than climate change and the niche shifting towards to cool climates (Polechová et al., 2009). Conversely, the model by Aguilée et al. (2016), which incorporates pollen dispersal, shows that species can persist under climate warming by spreading in space more slowly than the climate and adapting to warmer temperature. Such models are far from being fully understood from a mathematical standpoint (Champagnat and Méléard, 2007; Mirrahimi and Raoul, 2013). Indeed, sexual reproduction complicates the mathematical analysis and analytical predictions about spread rates were obtained only in situations where the leading and trailing edges shift at the same speed. We therefore lack results about spread rates when the species expands its distribution in the changing climate.

Models of joint spread in space and evolution of the niche in asexually reproducing organisms have been developed recently and are more amenable to mathematical analysis (Alfaro et al., 2013; Berestycki et al., 2016; Alfaro et al., 2017). In these models, a species can both track its favourable climate in space by dispersal and/or track the changing climate in time by evolving new phenotypic values by mutation, without the complicating effect of recombination. With asexual organisms, the finite range scenario set by the maladaptive swamping effect of gene flow at range margins described in Kirkpatrick and Barton (1997) does not occur and only two outcomes are predicted: the species either goes extinct everywhere or spread throughout space, but with a speed that can be fully characterized. The impact of climate change on the spread and adaptation of asexual organisms is also of interest in itself, since a large and important fraction of biodiversity (microbes in particular) reproduces mostly in a clonal manner. Many experimental tests of theoretical predictions about joint spatial spread and evolution furthermore use model clonal organisms in miniaturized landscapes (e.g. Bell and Gonzalez, 2011; Fronhofer and Altermatt, 2015; Larsen and Hargreaves, 2020). As the dynamics of range changes may differ between asexual and sexual organisms (Moerman et al., 2020), one therefore needs to produce theoretical predictions for the former to better interpret the results of these experiments.

We here build on recent mathematical results obtained in the case of asexual organisms colonizing a shifting spatial linear gradient (Alfaro et al., 2017), to discuss their biological implications in the context of climate change. We wish to predict (i) the critical velocity of climate change above which the species

goes extinct globally, (ii) if it does not go extinct globally, how fast it expands at its cold margin, (iii) whether it goes extinct locally at its warm margin, and how long it persists there (predicting the extent of the climatic debt). We also use the model to examine how adapting to local perturbations in the environmental gradient may block the spread of the species towards cooler climates and, conversely, how local improvement of habitat quality at the warm margin may help the species holding on its previous range. We generalize our predictions to the case of a species spreading in two dimensions.

2 Materials and methods

2.1 Model for a population in a 1D linear environment

We consider the density of an asexual population $n(t, x, y)$ at time $t \geq 0$, structured by a spatial variable $x \in \mathbb{R}$ (e.g. latitude) and a phenotypic trait $y \in \mathbb{R}$ (e.g. cold tolerance). It changes through four processes: dispersal, mutation, growth and competition. Dispersal and mutation are modelled by diffusion operators. We assume that the growth rate of the population at low density $r(t, x, y)$ declines as its phenotype y departs from a local optimum $y_{opt}(t, x)$, which varies across space along some environmental gradient (as temperature varies with latitude) and in time (as temperature warms due to climate change):

$$r(t, x, y) = r_{max}(x) - \frac{1}{2V_s} \left(y - y_{opt}(t, x)\right)^2, \tag{1}$$

where $r_{max}(x)$ is the maximal growth rate at x, and $\frac{1}{2V_s} > 0$ the strength of stabilizing selection around the optimal phenotype. In most sections (local perturbations are explored in Section 2.2), we further assume that the maximal growth rate is constant throughout space ($r_{max}(x) = r_{max}$) and that the optimal phenotype varies linearly through some dimension of space, with such optimal value also shifting in time at a constant speed due to climate change. More precisely,

$$y_{opt}(t, x) = b(x - ct), \tag{2}$$

where b describes the slope of the environmental gradient (how the optimal phenotype changes in space) and $c \geq 0$ describes the climate change velocity (how fast the location where a given phenotype is optimal shifts with time due to climate warming). We assume throughout that $b > 0$ and $c \geq 0$, but other scenarios of biological interest can be described by our model through an appropriate transformation of coordinates. Hence, the growth rate $r(t, x, y)$ is negative outside a strip centered on an optimal line $y = b(x - ct)$. Finally, we consider a logistic regulation of the population density such that competition depends on the total local density, but not on phenotypic resemblance among competitors.

The dynamics of $n(t,x,y)$ is described by the non local reaction-diffusion model:

$$\partial_t n(t,x,y) - \frac{\sigma^2}{2}\partial_{xx} n(t,x,y) - \frac{\mu^2}{2}\partial_{yy} n(t,x,y) = \left(r(t,x,y) - \frac{1}{k}\int_{\mathbb{R}} n(t,x,y')\, dy' \right) n(t,x,y), \qquad (3)$$

for $(t,x,y) \in \mathbb{R}_+ \times \mathbb{R}^2$. Here $\sigma > 0$, $\mu > 0$ describe the diffusion rates in geographical and phenotypic space, respectively. For simplicity, we will denote σ and $\mu > 0$ as the dispersal and mutation rates. The quantity $k > 0$ is the local (constant) carrying capacity.

Our first aim is to determine the maximal climate change velocity that the species can endure, thanks to a combination of dispersal and evolution. In case of survival, at time $t \geq 0$ and location x, the individual traits are concentrated around the optimal phenotypic trait, so that we can provide a simple macroscopic description of geographical distribution of the population by an interval $(x^-(t), x^+(t))$: if $x \in (x^-(t), x^+(t))$, the population is present in significant number and individual traits are close to $y_{opt}(t,x)$, while if $x \notin (x^-(t), x^+(t))$ the population is considered in too low numbers to be detectable. The position $x^-(t)$ thus corresponds to the warm edge of the species distribution, while $x^+(t)$ is the position of the cool edge of the geographical distribution. The core of the range at mid distance between $x^-(t)$ and $x^+(t)$ is denoted by $x^0(t)$. Our second aim is to fully characterize the speed at which these range edges and core shift in time.

We similarly define niche limits as $y^-(t)$ and $y^+(t)$, representing the most extreme phenotypic values found within the range. For instance, $y^-(t)$ would be the lowest cold tolerance (the warm niche limit), found at the warm edge of the range, and $y^+(t)$ the highest cold tolerance (the cool niche limit) at the cold edge of the range. The phenotypic value characterizing the center of the niche is noted $y^0(t)$. We will characterize the speed at which these niche limits and centre change in time (i.e. niche evolution).

Characterizing the velocity of these shifts in range and niche limits will allow us to define four scenarios of responses to climate change leading to population persistence (see Figure 1). We will examine under which conditions each of these scenarios occur and how they depend on, among others, the mutation and dispersal rates.

2.2 Model for a population in a more complex 1D environment

We consider more general situations with local environmental heterogeneity, affecting either the maximal growth rate or the optimal phenotype. In these cases, the bounds $x^-(t)$ and $x^+(t)$ do not move with constant speed any longer.

Impact of an obstacle. We consider the case where the population needs to cross an obstacle, e.g. a mountain, to expand towards the pole. The higher elevation implies colder temperatures, hence a steeper spatial gradient going up-slope than the latitudinal gradient. To keep on expanding towards the pole,

the species must also go down-slope, after having colonized the top elevation, where the environmental gradient changes sign locally: the population then needs to adapt to warmer (and not cooler) temperature while colonizing downhill (see Figure 2). To model this, we consider the growth function (1), with the optimal trait not given by (2) but

$$y_{opt}(t,x) = b(x - ct) + \varphi(x), \tag{4}$$

with $\varphi(x) \geq 0$ related to the elevation at x. Our question is: when is propagation towards the pole blocked by this obstacle?

Impact of a refuge. A second scenario is the presence of a refuge in a given location. We describe these enhanced growth conditions through a function $\psi(x) \geq 0$, which is positive on an interval. The growth function in (3) is then

$$r(t,x,y) = r_{max} + \psi(x) - \frac{1}{2V_s}\left(y - y_{opt}(t,x)\right)^2).$$

We consider a species which, in the absence of the refuge, would survive, but would escape towards the cooler part of the environmental gradient, thus disappearing from its original location, see Section 3.1 and Figure 1C-D. Our question is: can we avoid extinction at the warm edge by creating a local refuge (see Figure 3)?

2.3 Multidimensional version

To describe the dynamics of a population in a 2D environment, that is $\mathbf{x} = (x_1, x_2) \in \mathbb{R}^2$, we consider an extension of model (3), namely

$$\begin{aligned} \partial_t n(t,\mathbf{x},y) - \frac{\sigma^2}{2}\partial_{x_1x_1} n(t,\mathbf{x},y) - \frac{\sigma^2}{2}\partial_{x_2x_2} n(t,\mathbf{x},y) - \frac{\mu^2}{2}\partial_{yy} n(t,\mathbf{x},y) \\ = \left(r(t,\mathbf{x},y) - \frac{1}{k}\int_{\mathbb{R}} n(t,\mathbf{x},y')\,dy'\right) n(t,\mathbf{x},y), \end{aligned} \tag{5}$$

for $(t,\mathbf{x},y) \in \mathbb{R}_+ \times \mathbb{R}^2 \times \mathbb{R}$, where the linear environmental gradient depends only on the second coordinate x_2 of $\mathbf{x} = (x_1, x_2)$ (e.g. temperature varying with latitude but not longitude), that is

$$r(t,\mathbf{x},y) = r_{max} - \frac{1}{2V_s}(y - y_{opt}(t,\mathbf{x}))^2, \quad y_{opt}(t,\mathbf{x}) = b(x_2 - ct).$$

In this 2D context, the population is present on a set and the propagation of the range is anisotropic. We will determine in which the direction the propagation is the fastest.

3 Results

3.1 Dynamics of the population in a 1D linear environment

Conditions for survival or extinction. In S1, we show that, in the absence of climate change ($c = 0$), the survival or extinction of the population is decided by

$$R := r_{max} - \frac{1}{2}\sqrt{\frac{\mu^2 + b^2\sigma^2}{V_s}}, \tag{6}$$

which can be seen as the effective growth rate of the population at low density. The term $\frac{1}{2}\sqrt{\frac{\mu^2+b^2\sigma^2}{V_s}}$ can be interpreted as the fitness load caused by mutation and by dispersal along the spatial gradient. Indeed, both mutation and dispersal introduce individuals with non optimal phenotypes in any location. The effect of dispersal on the fitness load depends on both the typical dispersal distance σ and how fast selection changes when moving along the environmental gradient, as scaled by the slope b. If $R < 0$, the population is unable to survive, even without climate change. If $R > 0$, the population can survive if the speed of climate change is not too large. The critical speed of climate change is

$$c^{**} := \frac{\sqrt{2}}{b}\sqrt{\left(r_{max} - \frac{1}{2}\sqrt{\frac{\mu^2 + b^2\sigma^2}{V_s}}\right)(\mu^2 + b^2\sigma^2)} = \sqrt{2R}\sqrt{\sigma^2 + \frac{\mu^2}{b^2}}. \tag{7}$$

Climate change slower than c^{**} (that is $0 \leq c < c^{**}$) allows the population to survive, but climate change faster then c^{**} (that is $c > c^{**}$) leads to extinction. Formula (7) shows that the critical speed c^{**} for survival is a non-monotone function of σ and of μ (see also Figure 6): in one hand, increasing dispersal or mutation should allow better chances of survival because of, respectively, an increased capacity to track the shifting climate in space, and a faster evolution towards a greater thermal tolerance; on the other hand, higher mutation and dispersal increases the fitness load in every location. In our model, mutation and dispersal play similar roles on the critical speed for survival (i.e. c^{**} is a function of $\mu^2 + b^2\sigma^2$). They however have distinct effects on the speed at which the warm and cold edges of the range and niche change through time when the population persists.

Dynamics of the range. We consider a situation where the population is able to survive the climate shift, i.e. $R > 0$ and $0 < c < c^{**}$. Then, we find that the bounds $x^-(t)$ and $x^+(t)$ move at the constant speeds:

$$\frac{dx^-}{dt} = \frac{b^2\sigma^2}{\mu^2 + b^2\sigma^2}c - \sigma\mu\frac{b}{\mu^2 + b^2\sigma^2}\sqrt{(c^{**})^2 - c^2}, \tag{8}$$

$$\frac{dx^+}{dt} = \frac{b^2\sigma^2}{\mu^2 + b^2\sigma^2}c + \sigma\mu\frac{b}{\mu^2 + b^2\sigma^2}\sqrt{(c^{**})^2 - c^2}. \tag{9}$$

The core of the range shifts towards the cooler part of the environmental gradient (e.g. the pole) as

$$\frac{dx^0}{dt} = \frac{b^2\sigma^2}{\mu^2 + b^2\sigma^2} c. \tag{10}$$

This speed is always positive, but smaller than the climate change velocity (see purple lines in Figures 4 and 5). It approaches the speed of climate change as the mutation rate becomes small compared to the dispersal rate.

Dynamics of the niche. Since an individual can only survive at a given location if its phenotypic trait y is close to the local optimal phenotypic trait $y_{opt}(t, x)$, the spatial dynamics of the population is coupled to a dynamics of the niche, whose bounds move at the constant speeds:

$$\frac{dy^-}{dt} = b\left(\frac{dx^-}{dt} - c\right), \quad \frac{dy^+}{dt} = b\left(\frac{dx^+}{dt} - c\right). \tag{11}$$

The center of the niche evolves through time to be increasingly warm-adapted, as

$$\frac{dy^0}{dt} = -\frac{b\mu^2}{\mu^2 + b^2\sigma^2} c \tag{12}$$

is negative, decreasing when the climate change velocity or the mutation rate increase: evolution of the niche is faster when climate change is faster and when mutation rate is increasing relatively to dispersal (see purple lines in Figures 4 and 5).

Can the species track the shifting climate at the cold edge? Formula (9) shows that the cold edge of the population range always shifts towards the pole ($\frac{dx^+}{dt} > 0$), but it does so either slower or faster than the climate (see Figure 4): the cold edge shifts faster than climate ($0 \leq c < \frac{dx^+}{dt}$) if and only if $c < c^* < c^{**}$, where

$$c^* := \sqrt{2\left(r_{max} - \frac{1}{2}\sqrt{\frac{\mu^2 + b^2\sigma^2}{V_s}}\right)\sigma^2} = \sigma\sqrt{2R}. \tag{13}$$

In the absence of climate change and if $R > 0$, the population will ultimately expand and adapt to the entire gradient, with some speed of range expansion $\frac{dx^+}{dt} = \sqrt{2R}\frac{\sigma\mu}{\sqrt{\mu^2+b^2\sigma^2}}$ and niche expansion $\frac{dy^+}{dt} = b\frac{dx^+}{dt}$ (see Figure 4), which are limited by the capacity to adapt to different environmental conditions encountered when colonizing the climatic gradient. In particular, when the mutation rate is small, both the speed of range and niche expansion are slow. Climate change has a dual effect. In the one hand, the shifting climate makes conditions at the cool edge more similar to those already within the species niche, which tends to accelerate spatial spread at the cool edge of the range $\frac{dx^+}{dt}$. On the other hand, the speed of niche evolution at the cold margin $\frac{dy^+}{dt}$ always declines with increasing velocity of

climate change since it is harder to adapt to cooler climates when the climate warms rapidly (see Figure 4b). This slower adaptation to cool climates tends to slow down range expansion towards the pole $\frac{dx^+}{dt}$. The former effect dominates when climate change is not too large ($0 \leq c < c^*$), but the speed of range expansion towards cool climate declines with increasing velocity of climate change when $c > c^*$ due to constraints on adaptation at the cool edge of the niche. Interestingly, the speed of spatial propagation towards colder latitudes thus does not always increase with the speed of climate change (see Figure 4a).

Notice that the cold edge of the niche evolves to adapt to cooler temperatures (that is $\frac{dy^+}{dt} > 0$, see equation (11)), despite climate warming, if and only if $0 \leq c < c^*$, that is when the species range edge moves towards the pole faster than climate change. Conversely, when $c > c^*$, that is when the species spreads slower than climate change towards the pole, we have $\frac{dy^+}{dt} < 0$, meaning that the population gradually loses the ability to grow in the cooler part of its initial niche. Hence, if $c \in (c^*, c^{**})$, the population survives, shifts toward the pole, but fails to maintain its initial niche: the survival of the population then relies on its continual adaptation to warmer temperatures through mutations.

The speed of propagation towards the pole and the speed of niche expansion towards cooler climates first increase with increasing dispersal and mutation rates, but both speeds reach a maximum for some specific value of dispersal and mutation rates, above which propagation and niche expansion towards cool climates is slowed down by increasing dispersal and mutation loads (see Figure 5).

Can the species persist at the warm edge? When mutation is allowed ($\mu > 0$), the warm edge of the range always shifts towards the pole slower than the climate, i.e. $\frac{dx^-}{dt} < c$. Our model predicts continuous adaptation of the warm edge of the niche to warmer temperatures, as $\frac{dy^-}{dt} < 0$ always holds. Yet, the speed of adaptation is not necessarily sufficient to persist indefinitely at the warm edge of the range. Indeed, if $0 \leq c < c^{**}$, the speed of the warm edge of the population range $\frac{dx^-}{dt}$ can be either positive or negative, see (8). If $\frac{dx^-}{dt} > 0$, the population will disappear from the warmer part of its range and both the warmer and cold edge of the range will shift towards the poles, however at different speeds. This condition is met if the speed of climate change is higher than a critical climate velocity, but lower than the climate velocity causing extinction, i.e. when $c^\sharp < c < c^{**}$, where

$$c^\sharp := \frac{\mu}{b}\sqrt{2\left(r_{max} - \frac{1}{2}\sqrt{\frac{\mu^2 + b^2\sigma^2}{V_s}}\right)} = \frac{\mu}{b}\sqrt{2R}. \tag{14}$$

On the contrary, if climate change is not too fast and $c < c^\sharp < c^{**}$, then $\frac{dx^-}{dt} < 0$ and the warm edge of the range expands towards the opposite direction to climate change, thanks to mutations allowing fast evolution of the warm niche limit. The species can then persist in its initial range and holds on the previously warm edge of its distribution.

The speed at which the warm margin of the range shifts toward the pole always increases when climate change is faster (see Figure 4a). However, the speed at which the warm margin of the niche adapts to warmer temperature first increases when climate change is faster ($\frac{dy^-}{dt}$ is more negative), but it decreases when climate change is too fast (when $c > c^\sharp$) and the species disappears from its warm edge (see Figure 4b).

Both mutation and dispersal have antagonist effects on the speed of shift of the warm range margins. When dispersal or mutation are low and increase, it helps the population holding on its warm margin for longer. Yet, beyond some critical value, increasing dispersal or mutation has the reverse effect, making persistence at the warm margin more difficult. Interestingly, the dispersal and mutation rates maximizing the speed of propagation towards the pole differ from the values maximizing the persistence at the warm margin: in particular the dispersal rate maximizing the expansion towards the cool part of the gradient is greater than that minimizing retraction in the warm part of the gradient (see Figure 5a), while the mutation rate beyond which expansion towards the pole is slowed down is smaller than the value allowing the fastest expansion towards the equator (see Figure 5c).

Four scenarios of persistence under climate change. Depending on the values of the different parameters, both $c^* < c^\sharp$ and $c^\sharp < c^*$ may happen (see Figure 6). As a consequence the four scenarios described in Figure 1 are possible.

3.2 Dynamics of the population in a more complex 1D environment

3.2.1 Impact of a mountain

We consider a population expanding towards colder latitudes, and reaching a mountain. We assume $R > 0$ and $0 < c < c^{**}$, so that the population would survive in a linear environment and ask whether a local change in the slope of the environmental gradient $b + \varphi'(x)$ (see equation (4)) can stop the spatial spread. We show in Section S2.3 that different scenarios can lead to blocking at position x^{block}.

Spread halted when going uphill. Going uphill, blocking can happen if the population encounters a climatic gradient locally too steep to allow spread in a warming climate. This occurs at x^{block} when the speed of climate change is greater than

$$c^{**}_{\varphi'(x^{block})} = \frac{\sqrt{2}}{b}\sqrt{\left(r_{max} - \frac{1}{2}\sqrt{\frac{\mu^2 + (b+\varphi'(x^{block}))^2\sigma^2}{V_s}}\right)(\mu^2 + (b+\varphi'(x^{block}))^2\sigma^2)}. \qquad (15)$$

Expression (15) shows that a local increase in the slope of the gradient (as a steepened climatic gradient going uphill, see the blue line in Figure 7) has antagonistic effects on the capacity of the population

to keep spreading. In one hand, a steeper climatic gradient facilitates tracking the shifting climate in space, as shorter dispersal is then necessary to reach a favorable climate. On the other hand, a steeper climatic gradient generates a higher migration load depressing the population growth rate, even in a constant climate. As a result of these antagonistic effects, the critical climate change velocity has a local maximum for some intermediate value of the local environmental gradient $b + \varphi'(x^{block})$ (see Figure 7). Assuming that the population was able to spread until it hits the obstacle, it can be stopped, for the same climate change velocity, by a locally heightened climatic gradient going up-slope, because of the too large migration load there.

Spread halted when going downhill. Two different kinds of scenarios can halt the spread of a population that would have managed to reach the top of the obstacle, going downhill ($\varphi'(x^{block}) < 0$). In this case, the effect of the obstacle is to decrease the local slope of the environmental gradient, as b and $\varphi'(x^{block})$ have opposite signs.

The first scenario corresponds to the case where the presence of the obstacle locally weakens the latitudinal gradient, but does not change its sign (we still have $b+\varphi'(x^{block}) > 0$). The climate still cools when spreading towards higher latitude, but less so when going down-slope. The condition $c > c^{**}_{\varphi'(x^{block})}$ may then also occur when the local environmental gradient is small enough (see the green line in Figure 7). The environment becomes homogeneous and dispersal does not allow tracking the climate shift, which halts the spread of the population. In the latter case, a high mutation rate helps the population spread through these areas with shallow gradients under climate change (compare Figure 7a and Figure 7b).

The second scenario corresponds to the case where the obstacle is very steep with respect to the latitudinal gradient and locally inverts the local climatic gradient: $b + \varphi'(x^{block}) < 0$, i.e. the climate warms when going downhill. Even if the population has managed to spread uphill and the climate change velocity is below $c^{**}_{\varphi'(x)}$ for all location x, the population spread may then still be blocked when going downhill. We show that, if $\varphi'(x^{block}) < -b$, the population is only able to progress towards larger x if $0 \leq c < c^{\diamondsuit}_{\varphi'(x^{block})}$, where

$$c^{\diamondsuit}_{\varphi'(x^{block})} = \sqrt{2}b\sqrt{\frac{(b+\varphi'(x^{block}))^2\sigma^2}{\mu^2(\mu^2+(b+\varphi'(x^{block}))^2\sigma^2)^3} + \frac{1}{\mu^2+(b+\varphi'(x^{block}))^2\sigma^2}} \times \sqrt{r_{max} - \frac{1}{2}\sqrt{\frac{\mu^2+(b+\varphi'(x^{block}))^2\sigma^2}{V_s}}}. \quad (16)$$

Figure 7 (see the red line) shows how this second critical speed decreases when the local slope of the environmental gradient is more negative, going downhill. This blocking effect emerges from the double challenge of adapting to an inverted climatic gradient in a warming climate, locally making the situation

at the leading edge more similar to that at the warm edge of the range.

3.2.2 Impact of a refuge

We assume $R > 0$ and $c^\sharp < c < c^{**}$ so that the population succeeds to survive, but the rear edge of its range retreats towards colder temperatures. In the absence of a refuge, the population would then disappear from its original range. We however show in S2.4 that the population will succeed to maintain its presence in the refuge area at the warm edge of its range if and only if there exists a location x^{rescue} such that

$$\psi(x^{rescue}) > \frac{1}{2}\frac{b^2}{\mu^2}(c^2 - (c^\sharp)^2). \tag{17}$$

Unsurprisingly, higher local improvement of the quality of the environment in the refuge is necessary to maintain the population at its warm edge under faster climate warming (see Figure 8). Interestingly, the dispersal rate has only minor effects on the success of the refuge while increasing adaptation capacity through the mutation rate allows persistence in refuges of lower quality, consistently with our previous observation that mutation has larger effects on persistence at the warm edge than dispersal.

3.3 Dynamics of the population in a 2D linear environment

In a 2D setting, it is possible to show that, at large times, the range will evolve into an ellipse, which core, cold margin and warm margin move with the same velocities as in our 1D model (see section S3.2). Conditions for population survival, expansion of the niche at the cold edge and persistence at the warm margin of the range are therefore the same as previously.

The main difference introduced by a 2D setting is that the direction of faster spread of the range under climate warming does not necessarily correspond to the direction of climate change. To see this, let us consider the velocity of spread at every point along the edge of the range. We note as $\theta \in (0, 2\pi)$ the angle between the direction of range shift at the edge (orthogonal to the range edge at this point) and the direction of the climatic gradient, corresponding to the direction of the climate shift. When survival occurs, we show in S3.1 that the propagation is anisotropic: the speed in the θ-direction is

$$\omega_\theta := \sqrt{1 + b^2\frac{\sigma^2}{\mu^2}\sin^2\theta} \times \sigma\mu\sqrt{\frac{2r_{max} - \sqrt{\frac{\mu^2+b^2\sigma^2}{V_s}}}{\mu^2 + b^2\sigma^2} - \frac{b^2c^2}{(\mu^2 + b^2\sigma^2)^2}} + \cos\theta\frac{b^2\sigma^2}{\mu^2 + b^2\sigma^2}c. \tag{18}$$

Moreover, it turns out that when $c^* < c < c^{**}$, the largest ω_θ is obtained for $\theta = 0$, i.e. when the coldest point of the range shifts slower than climate, the direction of faster spread is also the direction of the climate shift. When $0 < c < c^*$, the largest ω_θ is obtained for some $0 < \theta_0 < \frac{\pi}{2}$, that can be exactly characterized. In this regime where the population spreads toward the pole faster than climate,

its range actually spreads faster in some different direction θ_0. Notice that $\theta_0 \to \frac{\pi}{2}$ as $c \to 0$.

In other words: when $c = 0$, the population spreads faster along a parallel where dispersing individuals changing only their longitude encounter an homogeneous environment. When c increases from 0 to c^* the fastest direction moves from "along a parallel" to "along a meridian", that is in the direction of the climate change. Then when c increases from c^* to c^{**} the faster direction remains "along a meridian", but the actual propagation speed of the population decreases until vanishing when $c = c^{**}$.

4 Discussion

Our model ignores many complexities of the real world affecting range and niche shifts under climate change, such as interspecific interactions, sexual reproduction and genetic drift. It however improves our understanding of these shifts by showing how allowing niche evolution along with spatial expansion is already sufficient to generate a large diversity of range shifts patterns, as observed in data. By providing simple closed-form expressions for range margins velocities, our model thus plays the same kind of heuristic role as classic reaction-diffusion models of the Fisher-Kolmogorov-Petrovsky-Piskunov type (Fisher, 1937; Kolmogorov et al., 1937) have played in structuring our predictions in the context of biological invasions when ignoring evolution. The present analytical predictions could in particular serve as baseline expectations when a species can both migrate and evolve to adapt to climate change, which could be compared to simulations and experimental data in more complex scenarios. Microcosms where dispersal and adaptation occur along environmental gradients (Moerman et al., 2020), where conditions change in time (Bell and Gonzalez, 2011), and in which the ability to disperse or to evolve can be manipulated (Szűcs et al., 2017) offer great opportunities to test our predictions.

Our model allows examining how evolutionary potential affects the patterns and speed of range changes in the context of a warming climate (see Thompson and Fronhofer, 2019, for simulations in sexual species). Interestingly, we predict that mutation and dispersal play symmetrical roles on the critical climate change velocity above which extinction is certain: to survive a species can track the changing climate either in geographical space by dispersing fast, or in phenotypic space by evolving fast. Both however have a cost because both mutation and dispersal in heterogeneous environment also continuously introduce maladapted genetic variation within populations, which, beyond some point, can slow down range expansion. While the population survival depends on the combined effect of mutation and dispersal, mutation rates per generation are typically orders of magnitude smaller than dispersal rates, which would suggest that mutation affects only marginally the prospects of persistence under climate change. Our expressions however show that the effect of dispersal is always scaled by the slope of the environmental gradient. When this gradient is relatively shallow compared to the typical dispersal

distance, comparing the phenotypic variation introduced by mutation and dispersal becomes less trivial. Fast evolution from de novo mutations is commonly observed in experiments with short-lived organisms in microcosms, with effects large enough to significantly affect extinction probability or spread rates in novel environments (Bell and Gonzalez, 2011; Szűcs et al., 2017). Fast evolution affecting range expansion in the context of climate change has also be documented in nature (Lustenhouwer et al., 2018; Colautti and Barrett, 2013). While evolutionary potential varies widely between species (in particular because of differences in generation time) and fast evolution is unlikely to be general, our model allows predicting how this variation may affect the diversity of responses to climate change.

Despite having similar effects on the overall persistence of the population, mutation and dispersal have distinct effects on patterns of range shift at the cool and warm edge of the species distribution. When evolutionary potential is non negligible, we predict faster velocities of range change at the cool edge than at the warm edge, as often documented in data (Ordonez, 2013), and in simulations with mutation and dispersal (Thompson and Fronhofer, 2019): increasing dispersal has a more positive effect on the range shift velocity at the cool edge, while increasing mutation allows populations to hold on their warm margins for longer and sometimes even to expand towards warmer climate in the direction opposite to climate change (as observed by Koide et al., 2022). When evolution permits niche shifts, our model also predicts that range shift velocity does not only differ between the leading and trailing edge, but also between the edges of the range and the core and that those velocities at the edges differ from the velocity of climate change in many situations where the population is still able to survive climate warming in the long term. Shifts at the core and edges of species range frequently differ also in data (Lenoir and Svenning, 2015). We predict both situations where the leading edge shifts faster than climate change, expanding its niche limits towards cooler climates (as observed by Lustenhouwer and Parker, 2022), and situations where its spreads slower than climate change, with niche contraction at the cool edge (as observed by Pardi et al., 2020). Our model shows that expectations about range shifts do differ depending on how and where these shifts are measured, which may explain why different empirical studies reach contradictory conclusions about climate tracking (Lenoir and Svenning, 2015).

Interestingly, we also predict that the velocity of shifts at the leading edge of the range does not always increase with the velocity of climate change and that, quite counter-intuitively, range shifts may actually slow down when climate change is too fast. A positive linear relationship between local climate change velocity and velocity of range shifts is often considered as evidence for impact of climate warming on species distributions (Chen et al., 2011; Lenoir and Svenning, 2015; Lenoir et al., 2020); yet, our model predicts that this relationship is neither expected to be linear, nor monotone, in general for the leading edge.

Extending our model to spatial spread in two dimensions also revealed that if the core of the range

is still expected to shift in the same direction as climate change, this is not necessarily true of spatial expansion at the edge: in particular the orientation of fastest spread at the edge is predicted to frequently differ from the direction of fastest climate change because strong environmental gradients tend to impede spatial expansion. Analysis of local climatic debts in the composition of communities at fine spatial scale (Gaüzère et al., 2017) frequently exhibit such discrepancies in the spatial orientation of shifts in local climate and species abundances: our model shows that parallel shifts are not necessarily expected, nor signal better persistence prospects in the long term.

Assuming asexual reproduction allowed us to derive explicit mathematical expressions for change in range and niche limits. Even though a large fraction of biodiversity affected by climate change does reproduce asexually most of the time (e.g. microbes), the majority of empirical data on range shifts in nature have been collected for species where sexual reproduction dominates. With sexual reproduction, the consequences of dispersal across environmental gradients may differ from those in an asexual species because of the phenomenon of "gene swamping": hybridization between locally adapted genotypes and immigrant genotypes makes it harder for selection to get rid of maladapted genes and asymmetric gene flow from the core of the range towards the margins can maintain the latter in a permanent state of maladaptation and low population size. As a result, while models of spread along environmental gradients of a single asexual species predict either extinction or unbounded range and niche expansion, similar models assuming sexual reproduction predict a third possible state where the species evolves a limited range, which shifts with climate change, but with the same velocity at the leading and rear edge (Pease et al., 1989; Polechová et al., 2009; Duputié et al., 2012; Aguilée et al., 2016). Both theoretical and empirical support for the role of gene swamping in setting range limits have however been challenged in recent years (Kottler et al., 2021), which casts doubts on the prevalence of this scenario of range shift in sexual species. We unfortunately lack precise mathematical predictions about the range edge velocities when a sexual species expands its range and niche, which is predicted to occur in a large range of conditions. It is interesting to note that our expression for the critical climate change velocity converges with that derived in sexual models (e.g Pease et al., 1989; Aguilée et al., 2016) for the case of limited ranges when the mutation rate is very low. Some mathematical models assuming sexual reproduction (Polechová et al., 2009; Aguilée et al., 2016) predict spread faster or slower than climate, with joint changes in niche limits. Our asexual model thus contributes to growing theory that suggests that niche shifts may often accompany range shifts in the context of climate change, making predictions about velocities of range changes more complex than previously assumed.

While niche evolution in our model allows a diversity of range shifts in response to climate change, other factors may ultimately be responsible for similar patterns in empirical data. Biotic interactions in particular, which are not considered in our simple model, are likely to explain a lot of variation in

range shifts in response to climate change, both at the warm and cold edge of the range (for empirical patterns and theoretical predictions respectively, see Paquette and Hargreaves, 2021; Thompson and Fronhofer, 2019). Changes in fundamental niche due to evolution and changes in realized niches due to dispersal limitation or altered biotic interactions are in practice very hard to discriminate in empirical data collected in the wild (Bates and Bertelsmeier, 2021). Feedbacks between range shifts and niche evolution, as occurs in our model, further make it difficult attributing a single cause to changes in distributions (Nadeau and Urban, 2019).

Our model shows how local perturbation of climatic gradients due to relief can stop the spread of a species towards higher latitude due to its inability to adapt to either too steep or inverted climatic gradients. We also predicted under which conditions local improvement of habitat quality can prevent extinction at the rear edge of the range. Many studies have examined how protected areas and their properties affect measures of climatic debt with sometimes contradictory conclusions (Bertrand et al., 2016; Gaüzère et al., 2016; Richard et al., 2021; Gaget et al., 2021, 2022). This diversity of findings may be due to the fact that climatic debt metrics at the community scale aggregates the effect of increased colonization rates by warm adapted species and that of decreased extinction of cold adapted local species in protected areas (Gillingham et al., 2015). Further mathematical developments now also allow to extend our analysis to nonlinear environmental gradients (Alfaro and Peltier (2022)), or different types of dispersal kernels.

Conclusion. We have provided simple predictions for range shifts at the leading and trailing edges of an asexual species surviving climate change by a combination of spatial tracking and niche evolution. Although our mathematical model is mostly of heuristic value at this stage, it draws attention to several important conclusions for nature conservation in the context of climate warming. First, variation in evolutionary potential may contribute to the large variation in observed and future range shifts. Second, management decisions anticipating extinction at the warm margin and range shifts there as fast as climate change may often be misled by the too simple expectation of climate tracking. Along the same line, our model suggests considering the notion of climatic debt in a nuanced way, as such a debt may not always signal threats on species persistence. Finally, our simple model predicts that conservation actions can have a long-lasting effect on range shifts when protected populations still have the capacity to adapt to new climates.

Acknowledgement. M.A. is supported by the *région Normandie* project BIOMA-NORMAN 21E04343. M.A. and G.R. are supported by the ANR project DEEV ANR-20-CE40-0011-01. G.R. is supported by the Chair "Modélisation Mathématique et Biodiversité" of Veolia Environnement-Ecole Polytechnique-Museum National d'Histoire Naturelle-Fondation X. O.R. acknowledges support from the France-Canada Research Funds (New Scientific collaboration Research program 2020) and the ANR project FloRes.The authors declare no conflicts of interest.

Authors contributions. M.A. and G.R. derived all the mathematical results, produced the figures, wrote the first version of the material and methods, results and supplementary material. O.R. discussed the biological interpretation and implications of the results, and the choice and presentation of figures with other authors, wrote the introduction and discussion and contributed to the writing of all other parts of the manuscript.

Data accessibility. There are no data associated with this manuscript. Equations provided in the main text and supplementary material allow reproducing all figures.

References

Aguilée, R., Raoul, G., Rousset, F., and Ronce, O. (2016). Pollen dispersal slows geographical range shift and accelerates ecological niche shift under climate change. *Proc. Natl. Acad. Sci. U.S.A.*, 113(39):E5741–E5748.

Alfaro, M., Berestycki, H., and Raoul, G. (2017). The effect of climate shift on a species submitted to dispersion, evolution, growth, and nonlocal competition. *SIAM J. Math. Anal.*, 49(1):562–596.

Alfaro, M., Coville, J., and Raoul, G. (2013). Travelling waves in a nonlocal reaction-diffusion equation as a model for a population structured by a space variable and a phenotypic trait. *Commun. Partial. Differ. Equ.*, 38(12):2126–2154.

Alfaro, M. and Peltier, G. (2022). Populations facing a nonlinear environmental gradient: steady states and pulsating fronts. *Math. Models Methods Appl. Sci.*, 32(2):209–290.

Angert, A. L., Crozier, L. G., Rissler, L. J., Gilman, S. E., Tewksbury, J. J., and Chunco, A. J. (2011). Do species' traits predict recent shifts at expanding range edges? *Ecol. Lett.*, 14(7):677–689.

Bates, O. K. and Bertelsmeier, C. (2021). Climatic niche shifts in introduced species. *Curr. Biol.*, 31(19):R1252–R1266.

Beissinger, S. R. and Riddell, E. A. (2021). Why are species' traits weak predictors of range shifts. *Annu. Rev. Ecol. Evol. Syst.*, 52(1):47–66.

Bell, G. and Gonzalez, A. (2011). Adaptation and evolutionary rescue in metapopulations experiencing environmental deterioration. *Science*, 332(6035):1327–1330.

Berestycki, H., Diekmann, O., Nagelkerke, C. J., and Zegeling, P. A. (2009). Can a species keep pace with a shifting climate? *Bull. Math. Biol.*, 71(2):399.

Berestycki, H., Jin, T., and Silvestre, L. (2016). Propagation in a non local reaction diffusion equation with spatial and genetic trait structure. *Nonlinearity*, 29(4):1434–1466.

Bertrand, R., Riofrio-Dillon, G., Lenoir, J., Drapier, J., De Ruffray, P., Gégout, J.-C., and Loreau, M. (2016). Ecological constraints increase the climatic debt in forests. *Nat. Commun.*, 7(1):1–10.

Case, T. J. and Taper, M. L. (2000). Interspecific competition, environmental gradients, gene flow, and the coevolution of species' borders. *Am. Nat.*, 155(5):583–605.

Champagnat, N. and Méléard, S. (2007). Invasion and adaptive evolution for individual-based spatially structured populations. *J. Math. Biol.*, 55(2):147.

588 Chen, I.-C., Hill, J. K., Ohlemüller, R., Roy, D. B., and Thomas, C. D. (2011). Rapid range shifts of
589 species associated with high levels of climate warming. *Science*, 333(6045):1024–1026.

590 Cobbold, C. A. and Stana, R. (2020). Should I stay or should I go: Partially sedentary populations can
591 outperform fully dispersing populations in response to climate-induced range shifts. *Bull. Math. Biol.*,
592 82(2):1–21.

593 Colautti, R. I. and Barrett, S. C. (2013). Rapid adaptation to climate facilitates range expansion of an
594 invasive plant. *Science*, 342(6156):364–366.

595 Davis, M. B., Shaw, R. G., and Etterson, J. R. (2005). Evolutionary responses to changing climate.
596 *Ecology*, 86(7):1704–1714.

597 Diamond, S. E. (2018). Contemporary climate-driven range shifts: Putting evolution back on the table.
598 *Funct. Ecol.*, 32(7):1652–1665.

599 Duputié, A., Massol, F., Chuine, I., Kirkpatrick, M., and Ronce, O. (2012). How do genetic correlations
600 affect species range shifts in a changing environment? *Ecol. Lett.*, 15(3):251–259.

601 Fisher, R. A. (1937). The wave of advance of advantageous genes. *Ann. Hum. Genet.*, 7(4):355–369.

602 Fronhofer, E. A. and Altermatt, F. (2015). Eco-evolutionary feedbacks during experimental range ex-
603 pansions. *Nat. Commun.*, 6(1):1–9.

604 Gaget, E., Johnston, A., Pavón-Jordán, D., Lehikoinen, A. S., Sandercock, B. K., Soultan, A., Božič, L.,
605 Clausen, P., Devos, K., Domsa, C., et al. (2022). Protected area characteristics that help waterbirds
606 respond to climate warming. *Conserv. Biol.*, 36(4):e13877.

607 Gaget, E., Pavón-Jordán, D., Johnston, A., Lehikoinen, A., Hochachka, W. M., Sandercock, B. K.,
608 Soultan, A., Azafzaf, H., Bendjedda, N., Bino, T., et al. (2021). Benefits of protected areas for
609 nonbreeding waterbirds adjusting their distributions under climate warming. *Conserv. Biol.*, 35(3):834–
610 845.

611 Gaüzère, P., Jiguet, F., and Devictor, V. (2016). Can protected areas mitigate the impacts of climate
612 change on bird's species and communities? *Divers. Distrib.*, 22(6):625–637.

613 Gaüzère, P., Princé, K., and Devictor, V. (2017). Where do they go? the effects of topography and
614 habitat diversity on reducing climatic debt in birds. *Glob. Change Biol.*, 23(6):2218–2229.

615 Gillingham, P. K., Bradbury, R. B., Roy, D. B., Anderson, B. J., Baxter, J. M., Bourn, N. A., Crick,
616 H. Q., Findon, R. A., Fox, R., Franco, A., et al. (2015). The effectiveness of protected areas in the
617 conservation of species with changing geographical ranges. *Biol. J. Linn. Soc.*, 115(3):707–717.

Hargreaves, A., Bailey, S., and Laird, R. A. (2015). Fitness declines towards range limits and local adaptation to climate affect dispersal evolution during climate-induced range shifts. *J. Evol. Biol.*, 28(8):1489–1501.

Kirkpatrick, M. and Barton, N. H. (1997). Evolution of a species' range. *Am. Nat.*, 150(1):1–23.

Koide, D., Yoshikawa, T., Ishihama, F., and Kadoya, T. (2022). Complex range shifts among forest functional types under the contemporary warming. *Glob. Change Biol.*, 28(4):1477–1492.

Kolmogorov, A., Petrovskii, I., and Piscunov, N. (1937). A study of the equation of diffusion with increase in the quantity of matter, and its application to a biological problem, byul. *Moskovskogo Gos. Univ*, 1(6):1–25.

Kottler, E. J., Dickman, E. E., Sexton, J. P., Emery, N. C., and Franks, S. J. (2021). Draining the swamping hypothesis: little evidence that gene flow reduces fitness at range edges. *Trends Ecol. Evol.*, 36(6):533–544.

Kubisch, A., Degen, T., Hovestadt, T., and Poethke, H. J. (2013). Predicting range shifts under global change: the balance between local adaptation and dispersal. *Ecography*, 36(8):873–882.

Larsen, C. D. and Hargreaves, A. L. (2020). Miniaturizing landscapes to understand species distributions. *Ecography*, 43(11):1625–1638.

Lenoir, J., Bertrand, R., Comte, L., Bourgeaud, L., Hattab, T., Murienne, J., and Grenouillet, G. (2020). Species better track climate warming in the oceans than on land. *Nat. Ecol. Evol.*, 4(8):1044–1059.

Lenoir, J., Gégout, J.-C., Guisan, A., Vittoz, P., Wohlgemuth, T., Zimmermann, N. E., Dullinger, S., Pauli, H., Willner, W., and Svenning, J.-C. (2010). Going against the flow: potential mechanisms for unexpected downslope range shifts in a warming climate. *Ecography*, 33(2):295–303.

Lenoir, J. and Svenning, J.-C. (2015). Climate-related range shifts–a global multidimensional synthesis and new research directions. *Ecography*, 38(1):15–28.

Lustenhouwer, N. and Parker, I. M. (2022). Beyond tracking climate: Niche shifts during native range expansion and their implications for novel invasions. *J. Biogeogr.*

Lustenhouwer, N., Wilschut, R. A., Williams, J. L., van der Putten, W. H., and Levine, J. M. (2018). Rapid evolution of phenology during range expansion with recent climate change. *Glob. Change Biol.*, 24(2):e534–e544.

MacLean, S. A. and Beissinger, S. R. (2017). Species' traits as predictors of range shifts under contemporary climate change: A review and meta-analysis. *Glob. Change Biol.*, 23(10):4094–4105.

Mirrahimi, S. and Raoul, G. (2013). Dynamics of sexual populations structured by a space variable and a phenotypical trait. *Theor. Popul. Biol.*, 84:87–103.

Moerman, F., Fronhofer, E. A., Wagner, A., and Altermatt, F. (2020). Gene swamping alters evolution during range expansions in the protist tetrahymena thermophila. *Biol. Lett.*, 16(6):20200244.

Moran, E. V. (2020). Simulating the effects of local adaptation and life history on the ability of plants to track climate shifts. *AoB Plants*, 12(1):plaa008.

Nadeau, C. P. and Urban, M. C. (2019). Eco-evolution on the edge during climate change. *Ecography*, 42(7):1280–1297.

Ordonez, A. (2013). Realized climatic niche of north american plant taxa lagged behind climate during the end of the pleistocene. *Am. J. Bot.*, 100(7):1255–1265.

Paquette, A. and Hargreaves, A. L. (2021). Biotic interactions are more often important at species' warm versus cool range edges. *Ecol. Lett.*, 24(11):2427–2438.

Pardi, M. I., Terry, R. C., Rickart, E. A., and Rowe, R. J. (2020). Testing climate tracking of montane rodent distributions over the past century within the great basin ecoregion. *Glob. Ecol. Conserv.*, 24:e01238.

Pease, C. M., Lande, R., and Bull, J. (1989). A model of population growth, dispersal and evolution in a changing environment. *Ecology*, 70(6):1657–1664.

Peischl, S. and Gilbert, K. J. (2020). Evolution of dispersal can rescue populations from expansion load. *Am. Nat.*, 195(2):349–360.

Peterson, M. L., Doak, D. F., and Morris, W. F. (2019). Incorporating local adaptation into forecasts of species' distribution and abundance under climate change. *Glob. Change Biol.*, 25(3):775–793.

Platts, P. J., Mason, S. C., Palmer, G., Hill, J. K., Oliver, T. H., Powney, G. D., Fox, R., and Thomas, C. D. (2019). Habitat availability explains variation in climate-driven range shifts across multiple taxonomic groups. *Sci. Rep.*, 9(1):1–10.

Polechová, J. (2018). Is the sky the limit? on the expansion threshold of a species' range. *PLoS biology*, 16(6):e2005372.

Polechová, J., Barton, N., and Marion, G. (2009). Species' range: adaptation in space and time. *Am. Nat.*, 174(5):E186–E204.

676 Polechová, J. and Barton, N. H. (2015). Limits to adaptation along environmental gradients. *Proc. Natl.*
677 *Acad. Sci. U.S.A.*, 112(20):6401–6406.

678 Potapov, A. B. and Lewis, M. A. (2004). Climate and competition: the effect of moving range boundaries
679 on habitat invasibility. *Bull. Math. Biol.*, 66(5):975–1008.

680 Richard, B., Dupouey, J.-l., Corcket, E., Alard, D., Archaux, F., Aubert, M., Boulanger, V., Gillet, F.,
681 Langlois, E., Macé, S., et al. (2021). The climatic debt is growing in the understorey of temperate
682 forests: Stand characteristics matter. *Glob. Ecol. Biogeogr.*, 30(7):1474–1487.

683 Szűcs, M., Vahsen, M., Melbourne, B., Hoover, C., Weiss-Lehman, C., and Hufbauer, R. (2017). Rapid
684 adaptive evolution in novel environments acts as an architect of population range expansion. *Proc.*
685 *Natl. Acad. Sci. U.S.A.*, 114(51):13501–13506.

686 Thompson, P. L. and Fronhofer, E. A. (2019). The conflict between adaptation and dispersal for main-
687 taining biodiversity in changing environments. *Proc. Natl. Acad. Sci. U.S.A.*, 116(42):21061–21067.

688 Weiss-Lehman, C. and Shaw, A. K. (2020). Spatial population structure determines extinction risk in
689 climate-induced range shifts. *Am. Nat.*, 195(1):31–42.

690 Wellenreuther, M., Dudaniec, R. Y., Neu, A., Lessard, J.-P., Bridle, J., Carbonell, J. A., Diamond,
691 S. E., Marshall, K. E., Parmesan, C., Singer, M. C., et al. (2022). The importance of eco-evolutionary
692 dynamics for predicting and managing insect range shifts. *Curr. Opin. Insect. Sci.*, page 100939.

693 Willis, K. and MacDonald, G. (2011). Long-term ecological records and their relevance to climate change
694 predictions for a warmer world. *Annu. Rev. Ecol. Evol. Syst.*, 42:267–287.

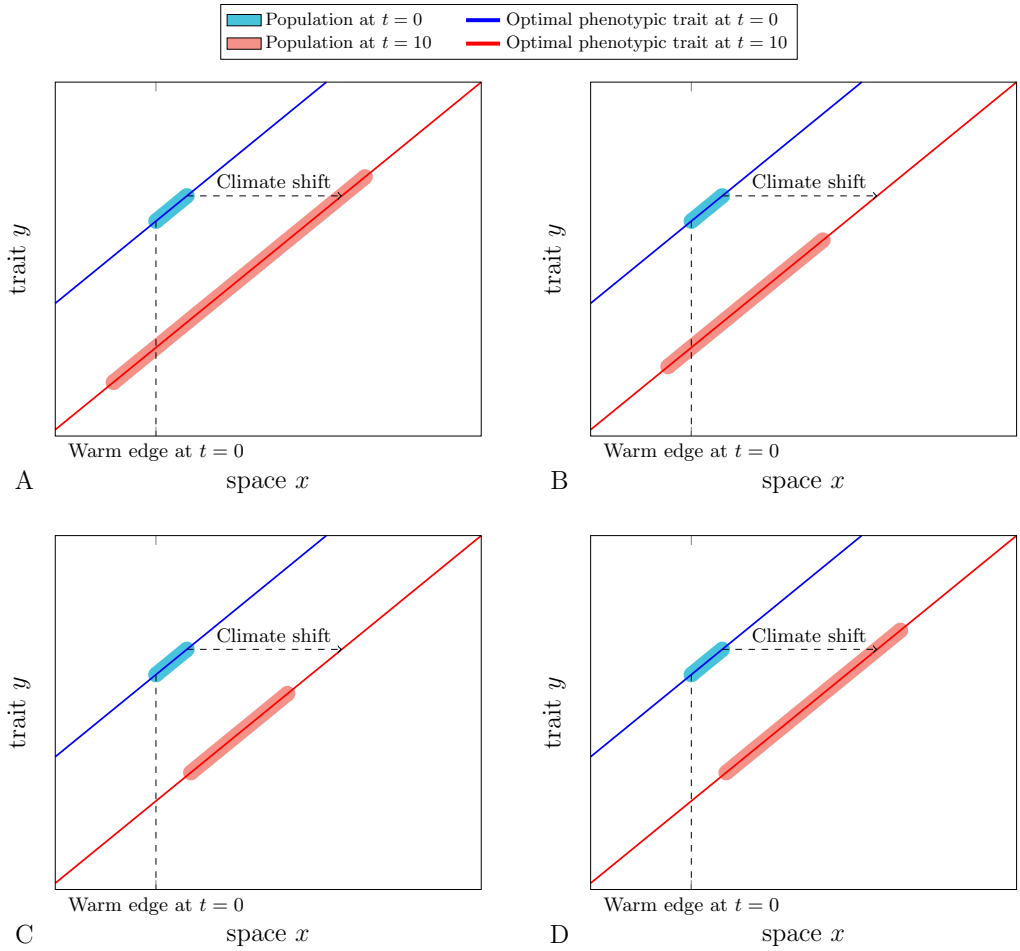

Figure 1: Four different possible scenarios of propagation. The population can expand towards the cooler part of the gradient at a velocity slower than that of climate change (B and C): in that case, it evolves a different cool niche limit, losing the ability to grow in the cooler climates to which it was previously adapted. Alternatively, the population can expand towards cool temperature faster than climate change velocity, colonizing cooler environments and adapting to colder climates than before (A and D). At the other side of the range, the species can go extinct locally at the warm edge (C and D), or, alternatively, it can evolve greater tolerance to warm temperature allowing holding on previously occupied range and even expanding towards warmer climates (A and B). The population maintains its initial range in A and B only, and it maintains its original niche in A and D only.

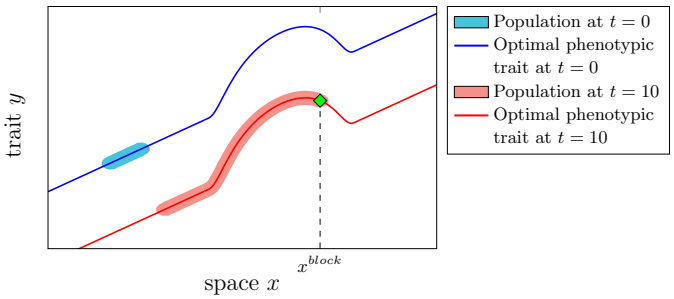

Figure 2: Geographical obstacle blocking the propagation. The population does not succeed to propagate past x^{block}, where the downhill slope of the mountain is too steep. Propagating downhill in the direction of the climate shift requires the population to adapt to the increase of temperature due to both climate change and the decreasing elevation.

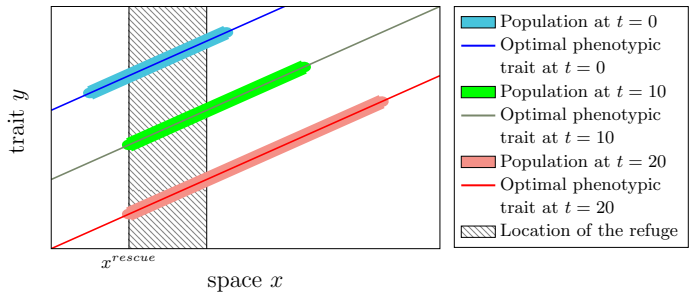

Figure 3: Effect of a refuge on extinction at the warm edge of the range. The population disappears from its warm edge until the position of the warm edge corresponds to a refuge at x^{rescue}, where the enhanced environment leads to the local survival of the population. This local survival is obtained through an adaptation to the increasing temperature. These heat resistant phenotypes, which can diffuse spatially, enable the population to survive locally also beyond the refuge.

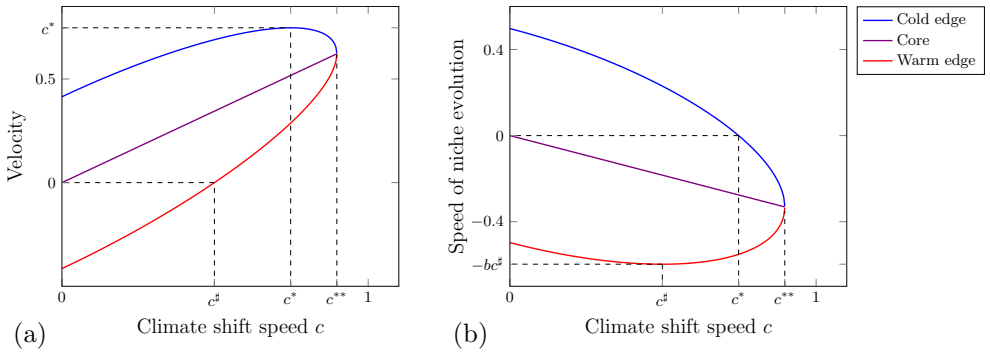

Figure 4: Range margins velocities and rate of evolution of niche margins as functions of the climate change velocity c. Blue lines: velocity $\frac{dx^+}{dt}$ of the cold margin of the population range in (a) and speed of evolution $\frac{dy^+}{dt}$ of the cold margin of the niche in (b). Red lines: velocity $\frac{dx^-}{dt}$ of the warm margin of the range in (a) and speed of evolution $\frac{dy^-}{dt}$ of the warm margin of the niche in (b). Violet line: velocity $\frac{dx^0}{dt}$ of the core of the range in (a) and speed of evolution $\frac{dy^0}{dt}$ of the core of the niche in (b). Here $r_{max} = V_s = \sigma = 1$, $b = 0.85$, $\mu = 0.8$.

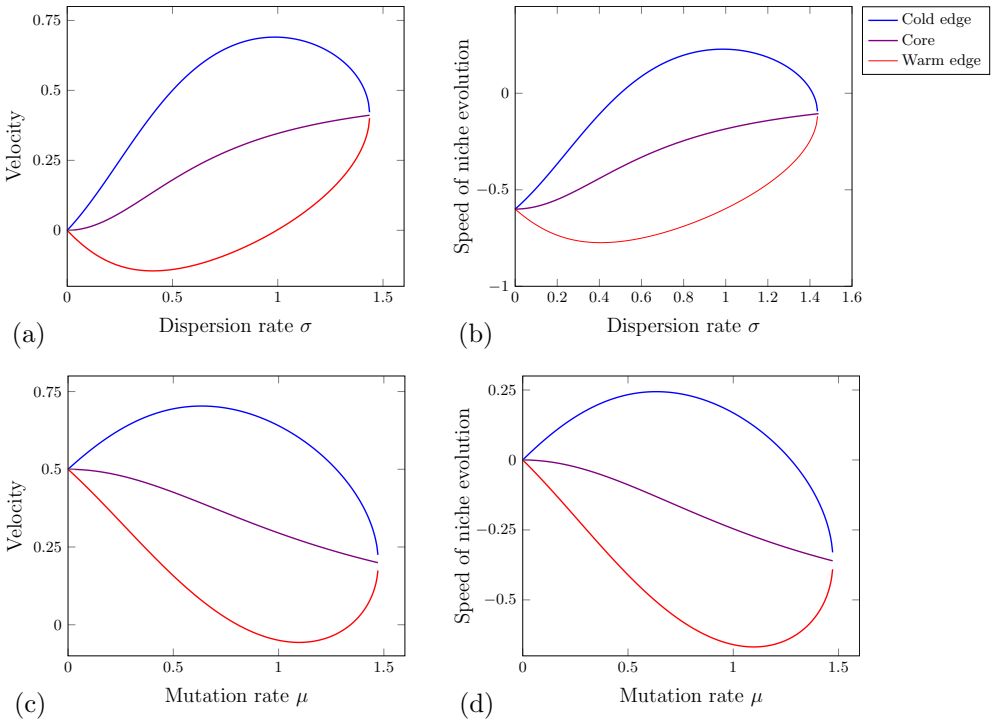

Figure 5: Range margins velocities and rate of evolution of niche margins as functions of dispersal and mutation rates. Top: Effect of variation in the dispersal rate σ. Here $r_{max} = V_s = 1$, $b = 0.85$, $\mu = 0.8$, $c = 0.5$. Bottom: Effect of variation in the mutation rate μ. Here $r_{max} = V_s = \sigma = 1$, $b = 0.85$, $c = 0.5$. Blue lines: velocity $\frac{dx^+}{dt}$ of the cold margin of the population range (a), (c), and speed of evolution $\frac{dy^+}{dt}$ of the cold margin of the niche (b), (d), red lines for the warm margin of the range (a), (c), and niche (b), (d) (i.e. $\frac{dx^-}{dt}$ and $\frac{dy^-}{dt}$ respectively). The violet line shows the speed of change in the core margin of the range (or niche) of the population (i.e. $\frac{dx^0}{dt}$ and $\frac{dy^0}{dt}$ respectively).

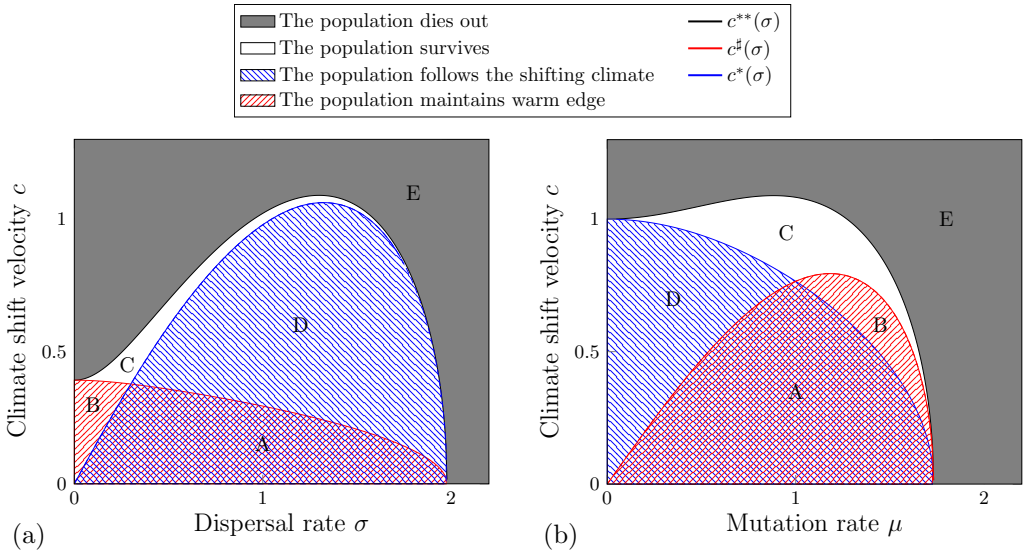

Figure 6: Description of the dynamics of populations for various dispersal rates $\sigma > 0$, mutation rates $\mu > 0$ and climate change speeds $c > 0$. Zone E: when the climate change speed is too fast, i.e. $c > c^{**}$, the population dies out. If the population survives (white area) and if the climate change speed is slow enough, the population may either maintain its warm edge (red area), succeed to maintain its phenotypic niche (blue area), or both. These various area are delimited by the critical climate change speeds c^{**}, c^{*} and $c^{\sharp}$ defined in Section 3.1. We obtain then four different dynamics of survival. Zone A: when $c < \min(c^{*}, c^{\sharp})$, the species both persists at the warm edge and tracks climate change in space at the cool edge, therefore surviving in its initial range and niche. This corresponds to Figure 1A. Zone B: when $c^{*} < c < c^{\sharp}$, the species survives in its initial range, but disappears from the cold edge of its niche. This corresponds to Figure 1B. Zone C: when $\max(c^{*}, c^{\sharp}) < c < c^{**}$ the species survives but disappears from the warm edge of its range and the cold edge of its niche. This corresponds to Figure 1C. Zone D: when $c^{\sharp} < c < c^{*}$, the species disappears from the warm part of its initial range, but tracks the shifting climate at the cooler range margin, thus surviving in its initial niche. This corresponds to Figure 1D. Here $b = r_{max} = V_s = 1$, and $\mu = 0.3$ in (a), $\sigma = 1$ in (b).

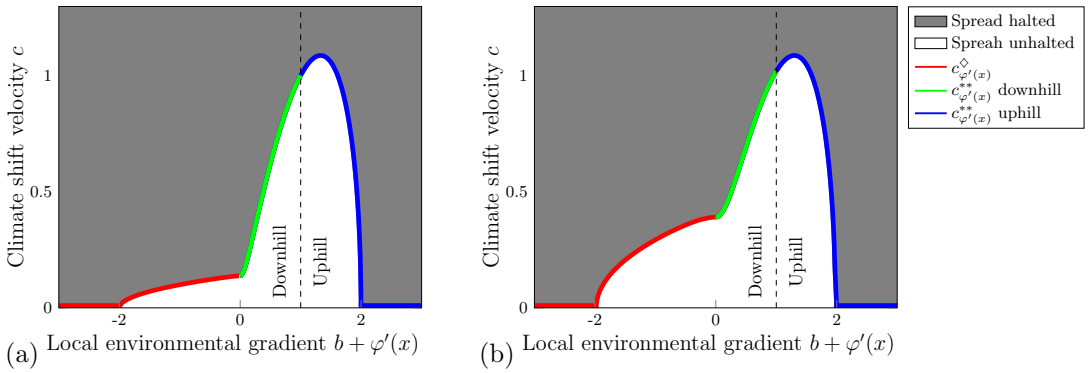

Figure 7: Effect of the mountain slope $\varphi'(x)$ with a climate shift speed $c \geq 0$. The gray area is where the population does not succeed to propagate in the direction of the climate shift, while this propagation is possible in the white area. Here $b = r_{max} = V_s = 1$, $\sigma = 1$, and $\mu = 0.1$ in (a), $\mu = 0.3$ in (b).

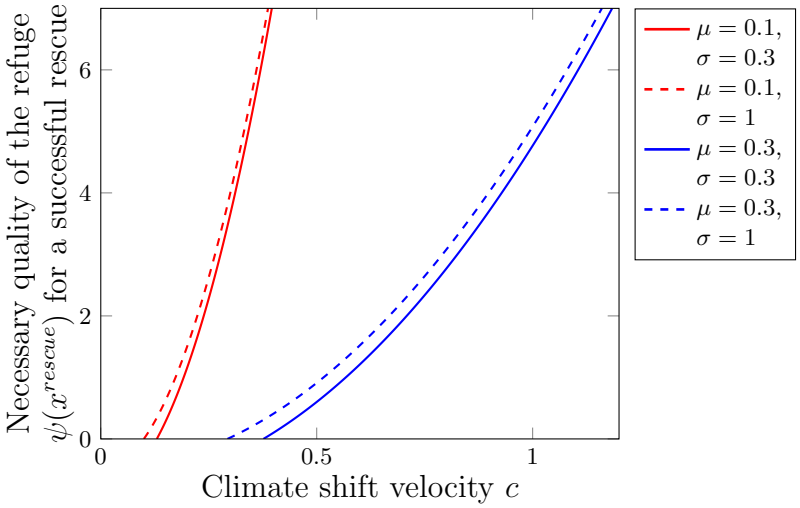

Figure 8: Necessary improvement of growth conditions in the refuge to allow persistence at the warm margin, as a function of climate change velocity $\psi(x^{rescue})$. Here $b = r_{max} = V_s = 1$.

- Supplementary Information -

When do leading and rear edges of the range shift slower or faster than climate? Insights from a mathematical model

S1 Speeds of propagation in a 1D linear environment

Here, as explained in the main text, the dynamics of the density $n(t,x,y)$ is described by the non local reaction diffusion model

$$\partial_t n(t,x,y) - \frac{\sigma^2}{2}\partial_{xx} n(t,x,y) - \frac{\mu^2}{2}\partial_{yy} n(t,x,y) = \left(r(t,x,y) - \frac{1}{k}\int_{\mathbb{R}} n(t,x,y')\,dy' \right) n(t,x,y), \tag{S1}$$

where the growth rate at low density is given by

$$r(t,x,y) = r_{max} - \frac{1}{2V_s}\left(y - y_{opt}(t,x)\right)^2, \tag{S2}$$

with the optimal phenotype given by

$$y_{opt}(t,x) = b(x - ct). \tag{S3}$$

To aggregate the coefficients that appear in (S1), we use the rescaling

$$N(T,X,Y) := \frac{1}{kr_{max}}\sqrt{\frac{\mu^2}{2r_{max}}}\, n\left(\frac{1}{r_{max}}T, \sqrt{\frac{\sigma^2}{2r_{max}}}X, \sqrt{\frac{\mu^2}{2r_{max}}}Y \right), \tag{S4}$$

where $n(t,x,y)$ solves (S1). Introducing this ansatz in equation (S1), one can check that $N(T,X,Y)$ solves

$$\partial_T N - \partial_{XX} N - \partial_{YY} N = \left(1 - A\left[Y - B(X - CT)\right]^2 - \int_{\mathbb{R}} N(T,X,Y')\,dY' \right) N, \tag{S5}$$

where

$$A := \frac{1}{2V_s}\frac{\mu^2}{2{r_{max}}^2}, \quad B := b\frac{\sigma}{\mu}, \quad C := c\sqrt{\frac{2}{r_{max}\sigma^2}}. \tag{S6}$$

Notice that c is the speed of the climate change in the original variables (t, x, y), whereas C is the speed of the climate change in the rescaled variables (T, X, Y).

Equation (S5) now falls into the mathematical analysis performed in Alfaro et al. (2013) when $C = 0$, and Section 4 of Alfaro et al. (2017) when $C > 0$. In particular, when $C = 0$, the condition for survival is

$$\lambda := \sqrt{A(1 + B^2)} - 1 < 0.$$

If this condition is satisfied, we define the critical speed

$$C^{**} := 2\sqrt{-\lambda\frac{1 + B^2}{B^2}}.$$

If $C > C^{**}$ then the population cannot endure the climate shift and goes extinct. If $C < C^{**}$ then the population will survive at all times, and moreover the size of the population range will increase. We can even describe the dynamics of the range with the speed of its leading and trailing edge, by defining

$$\Omega_X^- := -\sqrt{-\frac{4\lambda}{1 + B^2} - \frac{B^2}{(1 + B^2)^2}C^2} + \frac{B^2}{1 + B^2}C\,,$$

$$\Omega_X^+ := \sqrt{-\frac{4\lambda}{1 + B^2} - \frac{B^2}{(1 + B^2)^2}C^2} + \frac{B^2}{1 + B^2}C\,,$$

which are the propagation speeds in space X towards $-\infty$, $+\infty$ respectively. Similarly, we can compute the propagation speeds in the phenotypic space towards $-\infty$, $+\infty$:

$$\Omega_Y^- = B\Omega_X^- - BC, \quad \Omega_Y^+ = B\Omega_X^+ - BC.$$

To derive the formula of Section 3.1 of the main text, it is sufficient to introduce the original variables in these formula through (S6) and to notice that the rescaling (S4) implies

$$\frac{dx^\pm}{dt} = \sqrt{\frac{\sigma^2 r_{max}}{2}}\Omega_X^\pm, \quad \frac{dy^\pm}{dt} = \sqrt{\frac{\mu^2 r_{max}}{2}}\Omega_Y^\pm.$$

For instance, we collect

$$\frac{dx^-}{dt} = \frac{b^2\sigma^2}{\mu^2 + b^2\sigma^2}c - \sigma\mu\frac{b}{\mu^2 + b^2\sigma^2}\sqrt{(c^{**})^2 - c^2}, \tag{S7}$$

$$\frac{dx^+}{dt} = \frac{b^2\sigma^2}{\mu^2 + b^2\sigma^2} c + \sigma\mu \frac{b}{\mu^2 + b^2\sigma^2} \sqrt{(c^{**})^2 - c^2}. \tag{S8}$$

The effect of increasing speed of climate change, dispersal and mutation rates on the shifts of range and niche limits are discussed in the main text. Figure S1 shows that, quite trivially, increasing the population intrinsic rate of growth at low density, or decreasing the strength of stabilizing selection on the phenotype, facilitate both niche and range expansion at the cold and warm edge. The effect of increasing the slope of the environmental gradient is less trivial with antagonistic effects of spatial heterogeneity impeding niche and range expansion, but facilitating climate tracking.

By examining conditions under which $\frac{dx^+}{dt} > c$ and $\frac{dx^-}{dt} > 0$, we obtain expressions for the critical rate of climate change above which, respectively, the species fails to track its climatic niche in space (c^*), or fails to maintain the warm edge of its range ($c^\sharp$), as shown in the main text.

Comparison with critical climate change speeds from different models. In our model (see Section 3.1 of the main text), the critical speed for the climate shift speed c^{**}, above which the the species does not survive is

$$c^{**} = \frac{\sqrt{2}}{b} \sqrt{\left(r_{max} - \frac{1}{2} \sqrt{\frac{\mu^2 + b^2\sigma^2}{V_s}} \right) (\mu^2 + b^2\sigma^2)}\,. \tag{S9}$$

Letting $\frac{\mu}{b} \to 0$ — with $\mu^2 + b^2\sigma^2$ being constant— the critical speed for survival $c^{**} \to c^*$. In other words, a species with very low mutation can only survive by following the shifting climate. Notice also that letting $\frac{\mu}{b} \to 0$ — with $\mu^2 + b^2\sigma^2$ being constant— the critical speed for persisting at the warm edge of the range $c^\sharp \to 0$. In other words, a species with low evolutionary potential cannot maintain its warm edge.

Letting $\sigma \to 0$ — with $\mu^2 + b^2\sigma^2$ being constant— the critical speed for being able to follow the climate $c^* \to 0$. In other words, a species with very low dispersal cannot track the shifting climate. Notice also that letting $\sigma \to 0$ — with $\mu^2 + b^2\sigma^2$ being constant— the critical speed for survival $c^{**} \to c^\sharp$. In other words, a species with very low dispersal can only survive by adapting to warmer temperatures.

Formula (S9) can be compared to critical climate change speeds obtained from different models. Notice that we have derived other noteworthy formula in this study (for instance $\frac{dx^+}{dt}$, $\frac{dx^-}{dt}$, $\frac{dy^+}{dt}$, $\frac{dy^-}{dt}$, c^*, $c^\sharp$), which provide a more precise description of the dynamics, but we are not aware of related formula in other existing approaches.

In Berestycki et al. (2009), the authors have considered a situation with no evolution of individual traits. When considering the same type of growth rate function as here, the critical climate shift speed

they obtain is

$$c^{**}_{BDNZ} = \sqrt{2}\sqrt{\left(r_{max} - \frac{1}{2}\sqrt{2\frac{b^2}{2V_s}\sigma^2}\right)\sigma^2}.$$

One may then check that the critical speed c^{**}_{BDNZ} is coherent with the speed c^{**} given by (S9) when $\mu = 0$.

In models by (Pease et al., 1989; Polechová et al., 2009; Duputié et al., 2012; Aguilée et al., 2016), the population is described by its size and mean phenotypic trait at each time $t \geq 0$ and position $x \in \mathbb{R}$, under the assumption that the population is normally distributed in trait with a fixed phenotypic variance V_p. These assumptions are adequate for sexual populations when the evolving trait is highly polygenic and selection is weak (see Mirrahimi and Raoul (2013), where V_p is related to V_{LE}, the phenotypic variance at linkage equilibrium). Pease et al. (1989) and following models were able to derive a critical climate shift speed c^{**}_{TW} for a population with a limited range, above which extinction is certain (here shown with the same notations as ours):

$$c^{**}_{TW} = \frac{\sqrt{2}}{b}\sqrt{\left(r_{max} - \frac{1}{2}\sqrt{\frac{b^2\sigma^2}{V_s}}\right)b^2\sigma^2}, \tag{S10}$$

Note that this expression is derived by assuming that the phenotype is perfectly heritable as in the present manuscript. The phenotypic variance then disappears from the expression of the critical rate of climate change in those sexual models, which is just the same as in our asexual model when the mutation rate is null. A second type of population equilibrium, with an unlimited distribution, was considered in these models assuming sexual production (e.g. Polechová et al., 2009; Aguilée et al., 2016). A second critical climate change speed c^{**}_{UD} leading to extinction was derived in this situation:

$$c^{**}_{UD} = \frac{\sqrt{2}}{b}\frac{V_p}{\sqrt{V_s}}\sqrt{r_{max} - \frac{1}{2}\frac{V_p}{V_s}}, \tag{S11}$$

which does not depend on the dispersal rate σ. It is interesting to compare this critical climate change velocity to our expression in the asexual model when the dispersal rate is null:

$$c^{**}_{\sigma=0} = \frac{\sqrt{2}}{b}\mu\sqrt{r_{max} - \frac{1}{2}\sqrt{\frac{\mu^2}{V_s}}}, \tag{S12}$$

These critical climate change c^{**}_{TW} and c^{**}_{UD} were obtained in a model where the phenotypic variance of the population in any location is fixed, and it is this assumption that does not hold in our case: for our asexual model, the phenotypic variance is a dynamic quantity that results from the interplay of dispersal

($\sigma > 0$), mutation ($\mu > 0$), the environmental cline (b) and the strength of selection $\frac{1}{2V_s}$. This has two effects that reflect in (S9):

- In our model, mutations allow the population to evolve a resistance to heat and enhance their ability to survive. This is how we understand the last factor ($\mu^2 + b^2\sigma^2$) appearing in (S9). On the contrary, in the model developed in Pease et al. (1989), the limited range range equilibrium is stable only if the evolutionary potential (i.e. the phenotypic variance) is limited and thus, for c^{**}_{TW}, the species fail to take advantage of evolution and are bound to follow the climate change to survive. We believe this explains why the factor ($\mu^2 + b^2\sigma^2$) from (S9) becomes $b^2\sigma^2$ in (S10).

- The critical speed c^{**}_{UD} is obtained under the assumption that the population is uniformly present in the environment. The effect of the spatial structure then cancels out and the dynamics of the model is related to a non-spatial case. The non-spatial version of (S1) (i.e. this equation with $\sigma = 0$) leads to a phenotypic variance of $\tilde{V}_p = \mu\sqrt{V_s}$. We notice that with this ansatz, there is a coherence between (S9) and (S12).

S2 Speed of propagation in a more complex 1D environment

S2.1 Relevance of speed formula in non-linear environments

Real environments are more complex than the linear cases that we have considered above. Spatial heterogeneities range from small scales (e.g. the presence of rocks) to large scales (e.g. mountains). It is possible to introduce time and space dependence in the coefficients of our PDE model (Partial Differential Equation model, (S1)) to represent these features of the environment. Deriving quantitative properties of populations living in such environments is however a challenging task.

In Alfaro et al. (2017), a particular nonlinear environment was considered, and the dynamics of solutions was described. However the developed approach has limitations (that motivated us to adopt a different approach here): explicit speed formula are available in very few situations, and relying on a Partial Differential Equation (PDE) introduces artefacts. Indeed, the diffusion operators instantaneously bring infinitesimal populations everywhere and populations are thus never blocked.

In this manuscript, we thus decided to approximate the instantaneous propagation speed of a population by the speed of a corresponding linear environment. This idea has been developed in Maillard et al. (2021), using the residual effect of having a finite population size to describe explicitly the dynamics of the range of a population. This approximation is relevant to describe the impact of large heterogeneities, such as a mountain or a large refuge. It is however unable to capture the impact of precise properties of the environment, such as the effect of the area of a refuge.

S2.2 Speed of propagation in complex 1D case: beyond linear environments

We describe the spatial environment through the parameters $(t,x) \mapsto r_{max}$ and the optimal phenotypic trait $(t,x) \mapsto y_{opt}(t,x)$. If the heterogeneity is on a large scale compared to the dispersion scale of individuals, then the dynamics of the population can be investigated through the linear environment case studied in Section 3.1 of the main text, as explained above in S2.1. More precisely, this approximation will hold provided

$$\partial_t r_{max}, \quad \partial_x r_{max}, \quad \partial^2_{tt} y_{opt}, \quad \partial^2_{tx} y_{opt}, \quad \partial^2_{xx} y_{opt},$$

are small compared to $\sigma > 0$. Note that $\partial_t y_{opt}$ and $\partial_x y_{opt}$ do not need to be small compared to σ. Then, for (t,x) close to $(\bar{t},\bar{x})$, and provided $\partial_x y_{opt}(\bar{t},\bar{x}) \neq 0$, we have

$$r_{max}(t,x) \sim r_{max}(\bar{t},\bar{x}), \quad y_{opt}(t,x) \sim y_{opt}(\bar{t},\bar{x}) + \partial_x y_{opt}(\bar{t},\bar{x}) \left((x-\bar{x}) - \frac{-\partial_t y_{opt}(\bar{t},\bar{x})}{\partial_x y_{opt}(\bar{t},\bar{x})} \right).$$

If we denote $b(t,x) := \partial_x y_{opt}(\bar{t},\bar{x})$ and $c(t,x) := \frac{-\partial_t y_{opt}(\bar{t},\bar{x})}{\partial_x y_{opt}(\bar{t},\bar{x})}$, then the range $(x^-(t), x^+(t))$ evolves as follows:

$$\frac{dx^+}{dt}(t) := \sigma\mu \sqrt{\frac{2r_{max}(t,x^+(t)) - \sqrt{\frac{\mu^2 + b(t,x^+(t))^2\sigma^2}{V_s}}}{\mu^2 + b(t,x^+(t))^2\sigma^2} - \frac{b(t,x^+(t))^2 c(t,x^+(t))^2}{(\mu^2 + b(t,x^+(t))^2\sigma^2)^2}} + \frac{b(t,x^+(t))^2\sigma^2}{\mu^2 + b(t,x^+(t))^2\sigma^2} c(t,x^+(t)),$$

$$\frac{dx^-}{dt}(t) := -\sigma\mu \sqrt{\frac{2r_{max}(t,x^-(t)) - \sqrt{\frac{\mu^2 + b(t,x^-(t))^2\sigma^2}{V_s}}}{\mu^2 + b(t,x^-(t))^2\sigma^2} - \frac{b(t,x^-(t))^2 c(t,x^-(t))^2}{(\mu^2 + b(t,x^-(t))^2\sigma^2)^2}} + \frac{b(t,x^-(t))^2\sigma^2}{\mu^2 + b(t,x^-(t))^2\sigma^2} c(t,x^-(t)).$$

S2.3 Impact of a mountain

As explained in the main text, we here consider (S1), with the growth function (S2) and the optimal trait not given by (S3) but

$$y_{opt}(t,x) = b(x - ct) + \varphi(x). \tag{S13}$$

Here, $\varphi(x) \geq 0$ is related to the elevation at location x, and $\varphi(x) = 0$ outside of a given interval.

At time $\bar{t}$ let us denote by $x^+ = x^+(\bar{t})$, $y^+ = y^+(\bar{t})$ the position (in space and phenotype) of the front on the right side (i.e. the cool edge), whose instantaneous speed is under investigation. For $t = \bar{t} + \mathrm{d}\bar{t}$,

$x = x^+ + \mathrm{d}x^+$ and $y = y^+ + \mathrm{d}y^+$ we have

$$y - y_{opt}(t,x) = \mathrm{d}y^+ - (b + \varphi'(x^+))\mathrm{d}x^+ + bc\mathrm{d}\bar{t},$$

since $y^+ = y_{opt}(\bar{t}, x^+)$. Assuming that the dynamics is driven by the local environment, we use an analogy with the linear environment case studied in Section 3.1 of the main text. Therefore the instantaneous speed in space towards $+\infty$ can be obtained by letting $b \leftarrow b + \varphi'(x^+)$, $bc \leftarrow bc$ into formula (S8). This yields the following ordinary differential equation for the position of the front:

$$\begin{aligned} \frac{dx^+}{dt} &= \sigma\mu\sqrt{\frac{2r_{max} - \sqrt{\frac{\mu^2+(b+\varphi'(x^+))^2\sigma^2}{V_s}}}{\mu^2+(b+\varphi'(x^+))^2\sigma^2} - \frac{b^2c^2}{(\mu^2+(b+\varphi'(x^+))^2\sigma^2)^2}} \\ &\quad +\sigma^2\frac{bc}{\mu^2+(b+\varphi'(x^+))^2\sigma^2}(b+\varphi'(x^+)). \end{aligned} \tag{S14}$$

The population keeps spreading towards the pole when $\frac{dx^+}{dt}(t) > 0$. Examining the expression above shows that there are several distinct circumstances where such a spread rate towards the pole cannot be positive.

Let us consider situations where the population is halted at a point x^{block} in space, where the local gradient does not change sign. We thus have: $b + \varphi'(x^{block}) > 0$ (the climate locally cools down as the population expands towards the pole). The second term in (S14) is then positive. Yet, the first term in (S14) is not real if the quantity under the square root is negative. The spread of the population is then halted at x^{block} when the climate change velocity is higher than a critical speed, $c > c^{**}_{\varphi'(x^{block})}$ with:

$$c^{**}_{\varphi'(x^{block})} = \frac{\sqrt{2}}{b}\sqrt{\left(r_{max} - \frac{1}{2}\sqrt{\frac{\mu^2+(b+\varphi'(x^{block}))^2\sigma^2}{V_s}}\right)(\mu^2+(b+\varphi'(x^{block}))^2\sigma^2)}. \tag{S15}$$

This critical speed extends the definition of the quantity c^{**} to the case of local disturbance in the climatic gradient: we have in particular $c^{**}_{\varphi'(x^{block})} = c^{**}$ if $\varphi'(x^{block}) = 0$.

When the obstacle locally inverts the sign of the climatic gradient (e.g. going downhill a very steep mountain), the conditions for blocking the spread of the population towards higher latitude are different. When the local slope of the environmental gradient is negative enough ($\varphi'(x^{block}) + b < 0$), the second term in (S14) is then negative and the speed of propagation towards the pole $\frac{dx^+}{dt}(t)$ can vanish. If

$\varphi'(x^{block}) < -b$, the population is only able to progress towards larger x if $0 \le c < c^{\diamondsuit}_{\varphi'(x^{block})}$, where

$$c^{\diamondsuit}_{\varphi'(x^{block})} = \sqrt{2}b\sqrt{\frac{(b+\varphi'(x^{block}))^2\sigma^2}{\mu^2(\mu^2+(b+\varphi'(x^{block}))^2\sigma^2)^3} + \frac{1}{\mu^2+(b+\varphi'(x^{block}))^2\sigma^2}} \times \sqrt{r_{max} - \frac{1}{2}\sqrt{\frac{\mu^2+(b+\varphi'(x^{block}))^2\sigma^2}{V_s}}}. \tag{S16}$$

For a given climate shift speed c, this can be expressed in terms of a critical slope in the environmental gradient for which the population stops spreading: the population will not be able to propagate towards larger x provided

$$b + \varphi'(x^{block}) < -\frac{1}{\sigma}\sqrt{V_s\left(2r_{max} - \frac{b^2c^2}{\mu^2}\right)^2 - \mu^2}. \tag{S17}$$

S2.4 Impact of a refuge

As explained in the main text, we here consider (S1), with the growth function given by

$$r(t,x,y) = r_{max} + \psi(x) - \frac{1}{2V_s}\left(y - y_{opt}(t,x)\right)^2, \quad y_{opt}(t,x) = b(x-ct).$$

Here $\psi(x) \ge 0$ is related to the improvement of the environment in the refuge.

At time $\bar{t}$ let us denote by $x^- = x^-(\bar{t})$, $y^- = y^-(\bar{t})$ the position (in space and phenotype) of the front on the left side (i.e. the warm edge), whose instantaneous speed is under investigation. Assuming that the dynamics is driven by the local environment we get, as in S2.3, that the instantaneous speed in space towards $-\infty$ can be obtained by letting $r_{max} \leftarrow r_{max} + \psi(x^-)$. This yields the following ordinary differential equation for the position of the front:

$$\frac{dx^-}{dt} = -\sigma\mu\sqrt{\frac{2(r_{max}+\psi(x^-)) - \sqrt{\frac{\mu^2+b^2\sigma^2}{V_s}}}{\mu^2+b^2\sigma^2} - \frac{b^2c^2}{(\mu^2+b^2\sigma^2)^2}} + \frac{b^2\sigma^2}{\mu^2+b^2\sigma^2}c. \tag{S18}$$

From the assumption $c^\sharp < c < c^{**}$, the right hand side member in the above ODE is positive when $\psi \equiv 0$, meaning that the species will disappear from its original location. To prevent this, it suffices that there is a point x^{rescue} such that

$$-\sigma\mu\sqrt{\frac{2(r_{max}+\psi(x^{rescue})) - \sqrt{\frac{\mu^2+b^2\sigma^2}{V_s}}}{\mu^2+b^2\sigma^2} - \frac{b^2c^2}{(\mu^2+b^2\sigma^2)^2}} + \frac{b^2\sigma^2}{\mu^2+b^2\sigma^2}c < 0,$$

which is equivalent to

$$\psi(x^{rescue}) > \frac{1}{2}\frac{b^2}{\mu^2}(c^2 - (c^\sharp)^2). \tag{S19}$$

S3 Propagation in a 2D linear environment

As explained in the main text, to describe the dynamics of a population in a 2D environment, that is $\mathbf{x} = (x_1, x_2) \in \mathbb{R}^2$, we here consider an extension of model (S1), namely

$$\begin{aligned} &\partial_t n(t,\mathbf{x},y) - \frac{\sigma^2}{2}\partial_{x_1x_1} n(t,\mathbf{x},y) - \frac{\sigma^2}{2}\partial_{x_2x_2} n(t,\mathbf{x},y) - \frac{\mu^2}{2}\partial_{yy} n(t,\mathbf{x},y) \\ &\qquad = \left(r(t,\mathbf{x},y) - \frac{1}{k}\int_{\mathbb{R}} n(t,\mathbf{x},y')\,dy'\right) n(t,\mathbf{x},y), \end{aligned} \tag{S20}$$

where

$$r(t,\mathbf{x},y) = r_{max} - \frac{1}{2V_s}(y - y_{opt}(t,\mathbf{x}))^2, \quad y_{opt}(t,\mathbf{x}) = b(x_2 - ct).$$

Note that the environmental gradient is here assumed to be linear along the vertical axis.

S3.1 Speed of propagation in a 2D linear environment

Using again the rescaling (S4), with $n(t,\mathbf{x},y)$ solving (S20), we get that $N(T,\mathbf{X},Y)$ solves

$$\partial_T N - \Delta_{\mathbf{X}} N - \partial_{YY} N = \left(1 - A\left[Y - B(X_2 - CT)\right]^2 - \int_{\mathbb{R}} N(T,\mathbf{X},Y')\,dY'\right) N,$$

where A, B and C are given by (S6), and where $X_2 = \mathbf{X}\cdot\vec{e_2}$. In the basis $(\vec{e_1},\vec{e_2})$ the spatial coordinates are (X_1, X_2). We consider next any unit vector $\vec{\nu}$ in $\mathbb{R}^2$: we will consider populations with a density that only varies along the direction $\vec{\nu}$. Note that this direction does not necessarily align with the direction of the environmental gradient. To study such populations, the basis $(\vec{e_1'},\vec{e_2'}) = (\vec{\nu}, \mathrm{Rot}_{\frac{\pi}{2}}\vec{\nu})$ will be more convenient. The corresponding spatial coordinates are denoted (X_1', X_2') and if we denote by θ the angle from the direction of environmental gradient and $\vec{\nu}$ (ie $\nu = \mathrm{Rot}_\theta \vec{e_2}$), then

$$X_1' = \cos\theta\, X_2 + \sin\theta\, X_1, \quad X_2' = \sin\theta\, X_2 - \cos\theta\, X_1.$$

Hence, letting $N(T,X_1,X_2,Y) = \mathcal{N}(T,X_1',X_2',Y)$ we get

$$\partial_T \mathcal{N} - \Delta_{\mathbf{X}'}\mathcal{N} - \partial_{YY}\mathcal{N} = \left(1 - A\left[Y + D'X_2' - B'(X_1' - C'T)\right]^2 - \int_{\mathbb{R}} \mathcal{N}(T,\mathbf{X}',Y')\,dY'\right)\mathcal{N},$$

where

$$B' := B\cos\theta, \quad C' := \frac{C}{\cos\theta}, \quad D' = B\sin\theta.$$

Looking for solutions of the form

$$\mathcal{N}(T, X_1', X_2', Y) = \frac{1}{\sqrt{1+D'^2}} u\left(T, X_1', \frac{Y + D'X_2'}{\sqrt{1+D'^2}}\right),$$

we see that $u(T, X_1', Z)$ solves

$$\partial_T u - \partial_{X_1'X_1'} u - \partial_{ZZ} u = \left(1 - A_\theta \left[Z - B_\theta (X_1' - C_\theta T)\right]^2 - \int_{\mathbb{R}} u(T, X_1', Z')\, dZ'\right) u,$$

where

$$A_\theta := A(1+D'^2) = A(1 + B^2 \sin^2\theta), \quad B_\theta := \frac{B'}{\sqrt{1+D'^2}} = \frac{B\cos\theta}{\sqrt{1+B^2\sin^2\theta}}, \quad C_\theta := C' = \frac{C}{\cos\theta}. \tag{S21}$$

As in Section S1, the above equation falls into the mathematical analysis performed in Alfaro et al. (2013) and Section 4 of Alfaro et al. (2017). In particular, when $C_\theta = 0$, the condition for survival is

$$\lambda_\theta := \sqrt{A_\theta(1+B_\theta^2)} - 1 = \sqrt{A(1+B^2)} - 1 = \lambda < 0.$$

If so, then we define the critical speed

$$C_\theta^{**} := 2\sqrt{-\lambda \frac{1+B_\theta^2}{B_\theta^2}} = \frac{1}{\cos\theta} 2\sqrt{-\lambda \frac{1+B^2}{B^2}} = \frac{1}{\cos\theta} C^{**}.$$

On the one hand, if $C_\theta > C_\theta^{**}$ (which is equivalent to $C > C^{**}$) then the population cannot endure the climate shift and goes extinct. On the other hand, if $C_\theta < C_\theta^{**}$ (which is equivalent to $C < C^{**}$) the population will survive at all times, and moreover the size of the population range will increase.

We can describe the dynamics of the range in the θ-direction by defining

$$\begin{aligned} \Omega_\theta : &= \sqrt{-\frac{4\lambda}{1+B_\theta^2} - \frac{B_\theta^2}{(1+B_\theta^2)^2} C_\theta^2} + \frac{B_\theta^2}{1+B_\theta^2} C_\theta \\ &= \sqrt{1+B^2\sin^2\theta}\sqrt{-\frac{4\lambda}{1+B^2} - \frac{B^2}{(1+B^2)^2} C^2} + \cos\theta \frac{B^2}{1+B^2} C\,, \end{aligned} \tag{S22}$$

which is the propagation speed in the θ-direction given by $\vec{e_1'}$.

Now, let us investigate which direction θ maximizes the propagation speed Ω_θ. To do so, let us define, for $\theta \in [0, 2\pi)$,

$$\varphi(\theta) := \alpha \sqrt{1 + B^2 \sin^2\theta} + \beta \cos\theta,$$

where

$$\alpha := \sqrt{-\frac{4\lambda}{1+B^2} - \frac{B^2}{(1+B^2)^2}C^2}, \quad \beta := \frac{B^2}{1+B^2}C.$$

For $\theta \in [0,\pi]$, we notice that $\varphi(\theta) = \varphi(2\pi - \theta)$, and that for $\theta \in [0,\pi/2]$, $\varphi(\theta) > \varphi(\pi - \theta)$. We then simply need to find the maximum of $\varphi(\theta)$ for $\theta \in [0,\pi/2]$. Differentiating φ, we see that the sign of $\varphi'(\theta)$ is that of

$$\psi(\theta) := \alpha \cos\theta\, B^2 - \beta\sqrt{1 + B^2\sin^2\theta}.$$

ψ is decreasing (this can be checked by differentiating ψ), and $\psi(\frac{\pi}{2}) < 0$. We then simply need to consider the sign of $\psi(0) = \alpha B^2 - \beta$, which is actually given by the position of C with respect to

$$C^* := 2\sqrt{-\lambda}.$$

More precisely, if $C^* < C < C^{**}$, then $\psi(0) < 0$ and the speed is maximal in the $\theta = 0$-direction. On the other hand, if $0 < C < C^*$, then $\psi(0) > 0$ so that $\psi(\theta_0) = 0$ for a unique $0 < \theta_0 = \theta_0(C) < \frac{\pi}{2}$ given by $\cos\theta_0 \times B^2\alpha = \sqrt{1 + B^2\sin^2\theta_0} \times \beta$, that is

$$\cos\theta_0\sqrt{-\frac{4\lambda}{1+B^2} - \frac{B^2}{(1+B^2)^2}C^2} = \sqrt{1 + B^2\sin^2\theta_0}\,\frac{C}{1+B^2}.$$

The speed is then maximal in this θ_0-direction (and, equivalently, in the $2\pi - \theta_0$ region). Observe finally that $\theta_0 \to \frac{\pi}{2}$ as $C \to 0$.

Going back to the original variables through (S21), (S6) and

$$\omega_\theta = \sqrt{\frac{\sigma^2 r_{max}}{2}}\Omega_\theta,$$

we get the results of the main text. In particular, (S22) is recast

$$\omega_\theta := \sqrt{1 + b^2\frac{\sigma^2}{\mu^2}\sin^2\theta} \times \sigma\mu\sqrt{\frac{2r_{max} - \sqrt{\frac{\mu^2+b^2\sigma^2}{V_s}}}{\mu^2+b^2\sigma^2} - \frac{b^2c^2}{(\mu^2+b^2\sigma^2)^2}} + \cos\theta\frac{b^2\sigma^2}{\mu^2+b^2\sigma^2}c. \tag{S23}$$

S3.2 Dynamics of populations' range that are ellipses

Assume the environmental gradient is in the direction of $\vec{e_2}$. We look for an ellipse (describing the distribution of individuals) that is an exact solution to the dynamics given by (S23). At time $t \geq 0$, we consider the parametrization

$$\mathcal{E}(t) := \left\{(x_1(t) + L(t)\sin\xi, x_2(t) + \ell(t)\cos\xi) \in \mathbb{R}^2,\ 0 \leq \xi < 2\pi\right\}, \tag{S24}$$

of the ellipse of center

$$\mathbf{x}^0(t) = (x_1(t), x_2(t)) := (x_1^0, x_2^0 + vt),$$

with $v > 0$ to be determined, of semi-minor axis

$$\ell(t) := \ell_0 + \omega t,$$

with $\omega > 0$ to be determined, and of semi-major axis $L(t)$. We assume constant eccentricity $0 \leq e < 1$ so that $L(t) = \frac{1}{\sqrt{1-e^2}}\ell(t)$ which, for convenience, we write

$$L(t) = q\ell(t).$$

At a given time $t \geq 0$, consider a point $M(t) \in \mathcal{E}(t)$ "corresponding" to some $0 \leq \xi < 0$ (see the definition (S24) of the ellipse $\mathcal{E}(t)$). We denote $\vec{e_\theta} = (\sin\theta, \cos\theta)$ the outward unit normal vector to the convex envelop of $\mathcal{E}(t)$ at location $M(t)$. Note that the parameter ξ and θ are related through

$$\cos\theta = \frac{q}{\sqrt{\sin^2\xi + q^2\cos^2\xi}}\cos\xi, \quad \sin\theta = \frac{1}{\sqrt{\sin^2\xi + q^2\cos^2\xi}}\sin\xi. \tag{S25}$$

From this relation, we deduce

$$\frac{\cos^2\theta}{q^2} + \sin^2\theta = \frac{1}{\sin^2\xi + q^2\cos^2\xi}. \tag{S26}$$

The instantaneous propagation speed of the ellipse is given by

$$\vec{V}(t) = \frac{d}{dt}\overrightarrow{OM}(t) = (q\omega\sin\xi, v + \omega\cos\xi).$$

The speed of the propagation (in the direction normal to the edge of the range) is therefore

$$\vec{V}(t)\cdot\vec{e_\theta} = v\cos\theta + \omega(\cos\xi\cos\theta + q\sin\xi\sin\theta).$$

Using successively (S25) and (S26) this is recast

$$\begin{aligned}
\vec{V}(t)\cdot\vec{e_\theta} &= v\cos\theta + \omega\frac{q}{\sqrt{\sin^2\xi + q^2\cos^2\xi}} \\
&= v\cos\theta + \omega\sqrt{\cos^2\theta + q^2\sin^2\theta} \\
&= v\cos\theta + \omega\sqrt{1 + (q^2-1)\sin^2\theta}.
\end{aligned}$$

$\vec{V}(t) \cdot \vec{e_\theta}$ coincides with the target dynamics ω_θ in (S23). The ellipse will thus have an eccentricity e, its center will shift towards colder temperatures at a speed v and its semi-minor axe will grow at a speed ω, where

$$e = \sqrt{\frac{b^2\sigma^2}{\mu^2 + b^2\sigma^2}}, \quad v = \frac{b^2\sigma^2}{\mu^2 + b^2\sigma^2} c, \quad \omega = \sigma\mu \sqrt{\frac{2r_{max} - \sqrt{\frac{\mu^2+b^2\sigma^2}{V_s}}}{\mu^2 + b^2\sigma^2} - \frac{b^2c^2}{(\mu^2 + b^2\sigma^2)^2}}.$$

When the mutation rate is small compared to the dispersal rate, the population spreads more easily along spatial directions with homogeneous climate than in the direction of the climatic gradient: the eccentricity of the range is then close to one (the population spreads along longitude but is narrowly distributed in latitude). Note that, interestingly, our model predicts that the climate change velocity does not affect the shape of the range. The population will survive and expand when $\omega > 0$, which is the same condition as in our 1D model: in particular, R defined in (6) determines the survival (if $R > 0$) or extinction (if $R < 0$) of the population when there is no climate shift. When $R > 0$, the population will be able to survive a climate change provided the climate shift is smaller than the critical speed c^{**} defined in (S9). Notice that $\omega - v > 0$ means that the population will survive at its original location. Since $\omega - v$ has the same expression as $\frac{dx^-}{dt}$, in Section 3.1, the warmest point of the range of the population propagates towards warmer temperatures if $0 \leq c < c^\sharp$ (see Figure S2 (a)), and towards colder temperatures if $c > c^\sharp$ (see Figure S2 (b)). Similarly, the coldest point of the range shifts towards cooler climate at velocity $\omega + v$, which has the same expression as $\frac{dx^+}{dt}$, in Section 3.1, and thus higher than climate change velocity only when $0 \leq c < c^*$. The core of the range also moves towards cooler climates with the same speed as in our 1D model.

References

Aguilée, R., Raoul, G., Rousset, F., and Ronce, O. (2016). Pollen dispersal slows geographical range shift and accelerates ecological niche shift under climate change. *Proc. Natl. Acad. Sci. U.S.A.*, 113(39):E5741–E5748.

Alfaro, M., Berestycki, H., and Raoul, G. (2017). The effect of climate shift on a species submitted to dispersion, evolution, growth, and nonlocal competition. *SIAM J. Math. Anal.*, 49(1):562–596.

Alfaro, M., Coville, J., and Raoul, G. (2013). Travelling waves in a nonlocal reaction-diffusion equation as a model for a population structured by a space variable and a phenotypic trait. *Commun. Partial. Differ. Equ.*, 38(12):2126–2154.

Berestycki, H., Diekmann, O., Nagelkerke, C. J., and Zegeling, P. A. (2009). Can a species keep pace with a shifting climate? *Bull. Math. Biol.*, 71(2):399.

Duputié, A., Massol, F., Chuine, I., Kirkpatrick, M., and Ronce, O. (2012). How do genetic correlations affect species range shifts in a changing environment? *Ecol. Lett.*, 15(3):251–259.

Maillard, P., Raoul, G., and Tourniaire, J. (2021). Spatial dynamics of a population in a heterogeneous environment. *arXiv preprint arXiv:2105.06985*.

Mirrahimi, S. and Raoul, G. (2013). Dynamics of sexual populations structured by a space variable and a phenotypical trait. *Theor. Popul. Biol.*, 84:87–103.

Pease, C. M., Lande, R., and Bull, J. (1989). A model of population growth, dispersal and evolution in a changing environment. *Ecology*, 70(6):1657–1664.

Polechová, J., Barton, N., and Marion, G. (2009). Species' range: adaptation in space and time. *Am. Nat.*, 174(5):E186–E204.

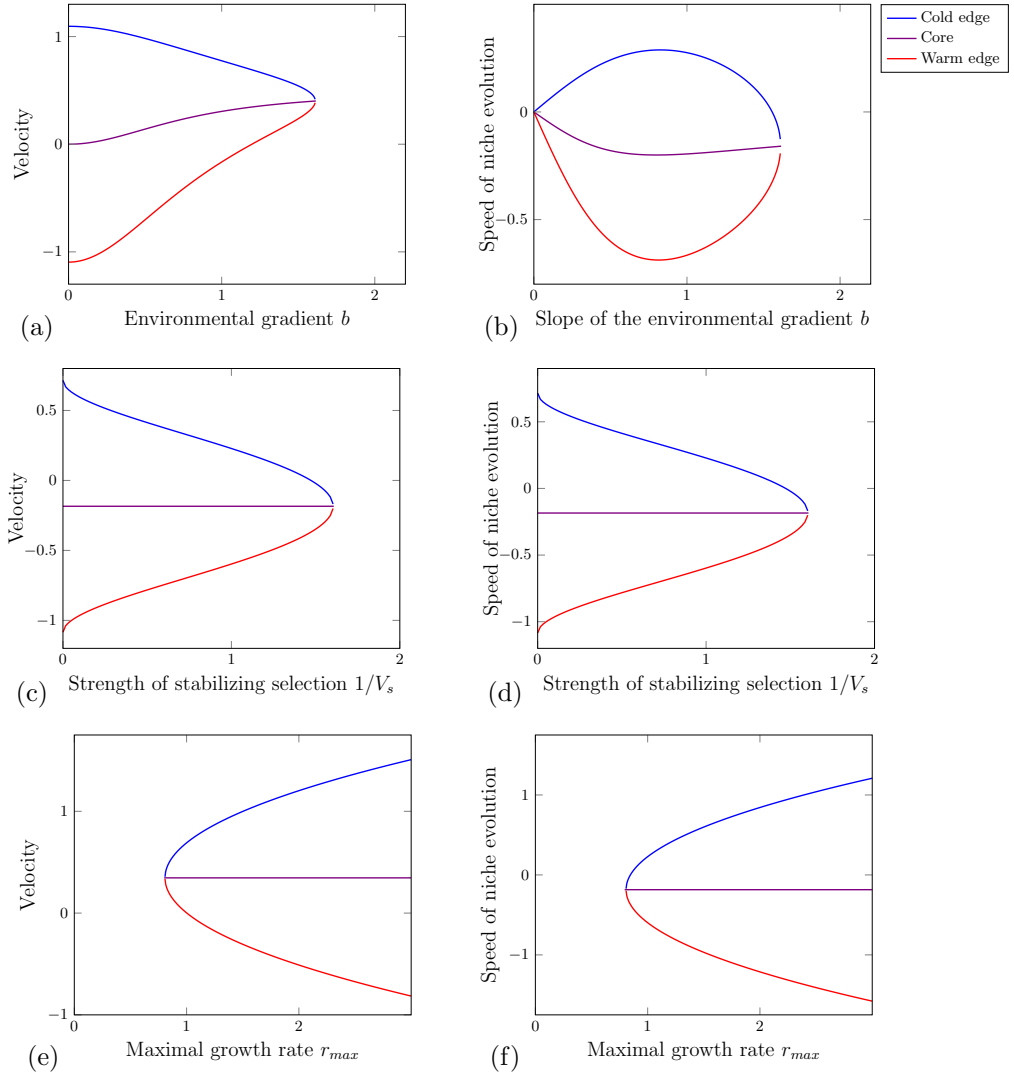

Figure S1: First line: Propagation velocity and evolutionary speed of the population as a function of the steepness of the environmental gradient b. Blue lines: velocity or speed of the edge of the population in the direction of the climate change ("northern edge"), red lines for the opposite edge. Violet lines for the velocity of the center of the range (left) and the evolutionary speed of the center of the phenotypic niche (right). Here $r_{max} = V_s = \sigma = 1$, $\mu = 0.8$, $c = 0.5$.
Second line: Propagation velocity and evolutionary speed of the population as a function of the strength of selection $\frac{1}{V_s}$. Here $r_{max} = \sigma = 1$, $b = 0.85$, $\mu = 0.8$, $c = 0.5$.
Third line: Propagation velocity and evolutionary speed of the population as a function of the maximal growth rate r_{max}. Here $V_s = \sigma = 1$, $b = 0.85$, $\mu = 0.8$, $c = 0.5$.

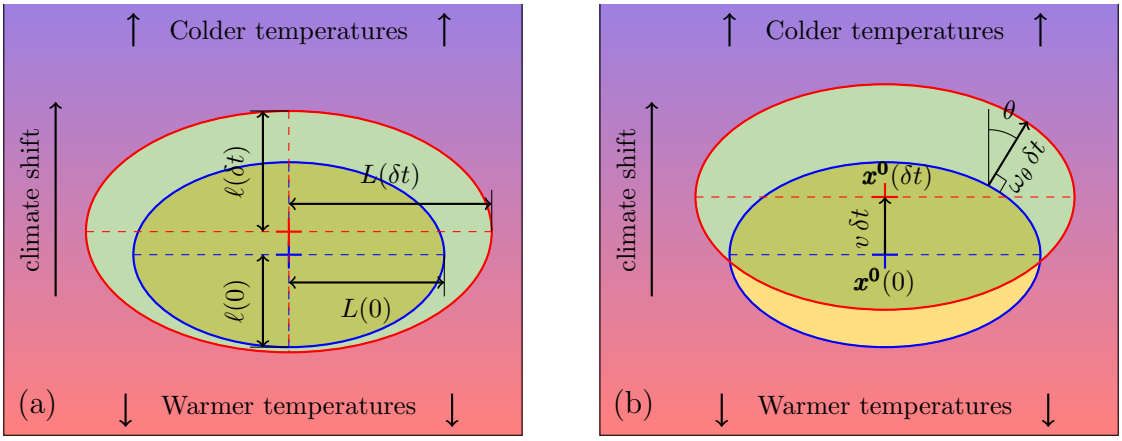

Figure S2: Dynamics of a range along an environmental gradient, with a climate shift speed $c = 0.4$ (left picture) and $c = 1$ (right picture). Warmer temperature in red and colder temperatures in blue, with the climate change shifting temperatures towards the top. The initial range ($t = 0$) of the species is the blue ellipse, and this range turns into the red ellipse at time $t = 30$. The time difference between the blue range and the red range is then $\delta t = 30$. On (a) we have indicated the notations for the semi-minor axis $l(t)$ and the semi-major axis $L(t)$. On (b) we have represented the shift of the core of the range $v\,\delta t$, and the propagation of a point of the edge of the range $\omega_\theta\,\delta t$. Here $r_{max} = 0.75$, $V_s = \sigma = 1$, $\mu = 0.1$, $b = 0.15$.